NASA MEMO 11-3-58L

NASA

MEMORANDUM

FORCE-TEST INVESTIGATION OF THE STABILITY AND CONTROL CHARACTERISTICS OF A 1/4-SCALE MODEL OF A TILT-WING VERTICAL-TAKE-OFF-AND-LANDING AIRCRAFT

By William A. Newsom, Jr., and Louis P. Tosti

Langley Research Center
Langley Field, Va.

NATIONAL AERONAUTICS AND SPACE ADMINISTRATION
WASHINGTON
January 1959

NATIONAL AERONAUTICS AND SPACE ADMINISTRATION

MEMORANDUM 11-3-58L

FORCE-TEST INVESTIGATION OF THE STABILITY AND CONTROL CHARACTERISTICS OF A 1/4-SCALE MODEL OF A TILT-WING VERTICAL-TAKE-OFF-AND-LANDING AIRCRAFT

By William A. Newsom, Jr., and Louis P. Tosti

SUMMARY

A wind-tunnel investigation has been made to determine the aerodynamic characteristics of a 1/4-scale model of a tilt-wing vertical-take-off-and-landing aircraft. The model had two 3-blade single-rotation propellers with hinged (flapping) blades mounted on the wing, which could be tilted from an incidence of 4° for forward flight to 86° for hovering flight.

The investigation included measurements of both the longitudinal and lateral stability and control characteristics in both the normal forward flight and the transition ranges. Tests in the forward-flight condition were made for several values of thrust coefficient, and tests in the transition condition were made at several values of wing incidence with the power varied to cover a range of flight conditions from forward-acceleration (or climb) conditions to deceleration (or descent) conditions The control effectiveness of the all-movable horizontal tail, the ailerons and the differential propeller pitch control was also determined. The data are presented without analysis.

INTRODUCTION

An investigation has been made of the stability and control characteristics of a 1/4-scale model of the Vertol 76 vertical-take-off-and-landing (VTOL) aircraft. The results of the free-flight tests of the model are reported in reference 1, and the results of the force tests are presented in the present paper.

The force tests included measurement of both longitudinal and lateral stability characteristics for the transition and normal-forward-flight conditions. The tests in the forward-flight condition were made at wing incidences of 4° and 14° for thrust coefficients from 0 through 0.5. The tests in transition flight were made for wing incidences from 20° through 80° with various power settings to represent conditions of steady level flight, forward acceleration (or climb), and deceleration (or descent). The control effectiveness of the all-movable horizontal tail was determined for both the forward-flight and transition conditions, and the effectiveness of the ailerons and the differential propeller pitch control was determined for the transition conditions.

SYMBOLS

The forces and moments are based on the stability-axis system, which is an orthogonal system with the origin at the airplane center of gravity. The Z axis is in the plane of symmetry and perpendicular to the relative wind, the X-axis is in the plane of symmetry and perpendicular to the Z-axis, and the Y-axis is perpendicular to the plane of symmetry.

F_L lift, lb

F_D drag, lb

M_Y pitching moment, ft-lb

F_Y side force, lb

M_X rolling moment, ft-lb

M_Z yawing moment, ft-lb

C_L lift coefficient, $\frac{F_L}{qS}$

C_D drag coefficient, $\frac{F_D}{qS}$

C_m pitching-moment coefficient, $\frac{M_Y}{qSc}$

C_Y side-force coefficient, $\frac{F_Y}{qS}$

C_l rolling-moment coefficient, $\frac{M_X}{qSb}$

C_n	yawing-moment coefficient,	$\frac{M_Z}{qSb}$
b	wing span, ft	

edge down, deg

ng edge down, deg

adius, deg

knots

ale flying model
light test inves-
rawing of the
s scaled up to the
ropellers with
ric motor which

ERRATA

NASA MEMO 11-3-58L

By William A. Newsom, Jr., and Louis P. Tosti
January 1959

Page 14:

In the title of figure 2(c) change $i_w = 4^\circ$ to $i_w = 14^\circ$.

Page 15:

In the title of figure 2(d) change $i_w = 14^\circ$ to $i_w = 4^\circ$.

Page 35:

In the title of figure 8(b) change V = 241 knots to V = 76 knots.

NASA - Langley Field, Va.

Issued 11-10-59

drove the propellers through shafting and right angle gear boxes. The speed of the motor was changed to vary the thrust of the propellers. The propeller blade angle was set at 12° except during the tests to determine the lateral control effectiveness of differential pitch of the two propellers.

The wing was pivoted at the 37-percent mean-aerodynamic-chord station and could be rotated to provide incidence of 4° to 86°. The model had an all-movable horizontal tail and conventional aileron and rudder controls for forward flight. Roll control in hovering flight was provided by varying the pitch of the propellers differentially. For pitch and yaw control in hovering flight, the model had jet reaction controls in the rear of the fuselage instead of the recessed tail "fans" in the horizontal and vertical tails which are used on the airplane, and the tail fans were not represented in the model tests.

TESTS

The tests were made in the Langley full-scale tunnel with the model support strut mounted near the lower edge of the entrance cone and about 5 feet above a ground board. Electric strain-gage balances were used to measure the forces and moments on the model and an electric tachometer was used to set the various model propeller speeds needed in the tests. Although during some of the tests, another model was left in the tunnel approximately 15 feet behind and slightly to the left of the present model, no corrections for flow angularity or blockage due to its presence have been applied to the data, since the blockage and interference effects were believed to be very small.

For the forward-flight condition, tests were made to determine the longitudinal stability and control characteristics and the lateral stability characteristics for thrust coefficients from 0 to a value of 0.5 which represented full power at a lift coefficient of 1.0. These tests were made with a wing incidence of 14° as well as with the design incidence of 4°. The longitudinal stability tests covered a range of angles of attack from -5° to 20° and tail incidences from 0° to -15°. The lateral stability tests covered a range of sideslip from -20° to 20° and angles of attack from 0° to 20°.

For the investigation of the transition-flight condition, tests were made for a range of power settings from that required for a forward acceleration of 1/2g or a rate of climb of 500 feet per minute for the full-scale aircraft (whichever was the greater) to that required for a deceleration of 1/2g or a rate of descent of 500 feet per minute (whichever was the less). For tests at wing incidences of 20°, 40°, and 60°, the forward acceleration or deceleration proved to be the determining condition and the tests were made with power settings which, with the

fuselage at zero angle of attack, gave forward accelerations of 1/2g and 1/4g, zero acceleration, and decelerations of 1/2g and 1/4g. With these power settings, the angle of attack was varied for longitudinal stability and control tests from -15° to 20° with the stabilizer off and with the stabilizer set at various angles of incidence from 0° to 15°. Lateral stability and control tests at wing incidences of 20°, 40°, and 60° were made with power settings which gave forward accelerations of 1/4g, 0, and -1/4g with the fuselage at angles of attack of 0° and 10°. These tests covered a range of sideslip angles from 20° to -20°, deflections of the right aileron from 30° to -30°, and total differential propeller pitch from 0° to 6° (for the condition of zero acceleration at $\alpha = 0°$ only).

For a wing incidence of 80°, the condition for rate of climb of 500 feet per minute required the greater power variation, and the tests were consequently set up to represent the climb and descent conditions. Tests were made with the power settings for steady level flight with the fuselage at 0° angle of attack, for a 45° climb or descent with the fuselage level (angle of attack, -45° or 45°, respectively), and for a 26.5° climb or descent with the fuselage level. For the longitudinal stability and control tests, the fuselage angle of attack was varied approximately ±10° from these conditions with the horizontal tail off and with the tail on at angles of incidence of 0° and 15°. Tests were made at sideslip of 20° to -20°, and aileron-effectiveness tests were made with the fuselage level for a range of deflection of the right aileron from 30° to -30° for the level-flight, the 26.5° climb, and the 26.5° descent power conditions. The effectiveness of the differential propeller pitch control was determined only for the level flight condition.

The tests at wing incidences of 4° and 14° were made at an airspeed of about 29 knots, which gave an effective Reynolds number based on the wing chord and free-stream velocity of about 400,000. For the tests at higher angles of wing incidence it was necessary to reduce the tunnel airspeed below 29 knots to avoid exceeding the model motor limitations. The Reynolds number based on the wing chord and slipstream velocities varied between 200,000 and 750,000.

PRESENTATION OF RESULTS

The results of the force test investigation to determine the aerodynamic characteristics of a 1/4-scale model of the Vertol 76 VTOL aircraft are presented in figures 2 to 14. The data for the normal forward flight tests ($i_w = 4°$ and 14°) are presented in coefficient form, but since the coefficients approach infinity and become essentially meaningless as the velocity approaches zero, the data for the transition flight tests ($i_w = 20°$, 40°, 60°, and 80°) have been scaled up to the weight

and center-of-gravity locations of the full-scale airplane listed in table II. It should be noted, however, that although the data have been scaled up to correspond to the weight values of table II for tests made at power settings that gave zero net drag and acceleration or deceleration of 1/4g and 1/2g at $\alpha = 0^\circ$, the data can be interpolated and rescaled in terms of other conditions such as climb or glide or trim at other angles of attack. If the data are rescaled, all forces and moments are simply multiplied by the factor required to make the lift equal to the desired value for the desired condition, and the velocity is multiplied by the square root of this factor. All tests were made with a mean blade angle of 12° instead of a blade angle adjusted to the proper value for each condition, since the variation of rotor speed and blade angle for the airplane was not known. Instead of adjusting the blade angle, the propeller speed was adjusted to give the proper thrust and, consequently, the proper slipstream velocity and position for each test condition.

All the data of figures 2 and 3 were obtained at the normal forward flight conditions ($i_w = 4^\circ$ and 14°, $T_c' = 0$, 0.25, and 0.50). Figure 2 shows the variation of lift coefficient, drag coefficient, and pitching-moment coefficient with angle of attack, and figure 3 shows the variation of rolling-moment coefficient, yawing-moment coefficient, and side-force coefficient with sideslip angle. During each test, horizontal-tail deflections of 0°, -10°, and -15° were used, and data were also obtained with the horizontal tail off.

The data obtained in the tests through the transition flight range are presented in figures 4 to 11. In figures 4 to 8 are plots presenting the variation of lift, drag, and pitching moment with angle of attack at several horizontal tail deflections, the separate figures representing the different flight conditions of zero acceleration and of both acceleration and deceleration of 1/4g and 1/2g. Figure 9 shows data obtained for the variation of lift, drag, and pitching moment with angle of attack for the climbing and descending flight conditions with 80° wing incidence. For figure 9(a) the model was set at $\alpha = -26.5^\circ$ and the 26.5° climb (or forward acceleration of 1/2g) condition was established. The angle of attack was then varied up and down from -26.5° for the tests. The data of figure 9(b) represent a 45° climb (or acceleration of 1 g) and the test conditions were set up in a manner similar to those discussed for figure 9(a). The condition for a 26.5° descent angle was represented by establishing 1/2g of deceleration at $\alpha = 26.5^\circ$ and a 45° descent angle was represented by a deceleration of 1 g at $\alpha = 45^\circ$ (figs. 9(c) and 9(d)). Figure 10 shows the variation of rolling moment, yawing moment, and side force with sideslip angle for wing incidences of 20°, 40°, 60°, and 80°. The tests were for the conditions of zero acceleration and for accelerating or decelerating flight of 1/4g at both $\alpha = 0^\circ$ and $\alpha = 10^\circ$. The lateral stability data for a wing incidence of 80° and a 45° climb (acceleration of 1 g) are presented in figure 11. The results of the tests of the lateral control effectiveness through the

transition flight range are presented in figures 12 to 14. In figures 12 and 13, the effect of deflection of the right aileron on the rolling moment, yawing moment, and side force is presented, and figure 14 shows the effect of differential propeller pitch.

CONCLUDING REMARKS

Data have been presented for a 1/4-scale model of a vertical-take-off-and-landing aircraft with a wing capable of being tilted from 4° incidence for forward flight to 86° incidence for hovering flight. Included are longitudinal and lateral stability data covering a range of conditions simulating zero forward acceleration and accelerating and decelerating flight in level, climbing, and descending flight.

Langley Research Center,
National Aeronautics and Space Administration,
Langley Field, Va., October 2, 1958.

REFERENCE

1. Tosti, Louis P.: Flight Investigation of the Stability and Control Characteristics of a 1/4-Scale Model of a Tilt-Wing Vertical-Take-Off-and-Landing Aircraft. NASA MEMO 11-4-58L, 1959.

TABLE I.- SCALED-UP GEOMETRIC CHARACTERISTICS OF THE MODEL

Propellers (3 blades each rotor):	
Diameter, ft	9.33
Solidity	0.239
Chord, ft	1.0
Wing:	
Pivot, percent chord	37
Sweepback (leading edge), deg	0
Airfoil section	NACA 4415
Aspect ratio	5.42
Chord, ft	4.75
Taper ratio	1.0
Area, sq ft.	118.2
Span, ft	24.88
Dihedral angle, deg	0
Ailerons (each):	
Chord, ft	1.22
Span, ft	4.83
Hinge line, percent chord	74.1
Vertical Tail:	
Sweepback (leading edge), deg	0
Airfoil section	NACA 0012
Aspect ratio	1.25
Chord, ft	4.0
Taper ratio	1.0
Area, sq ft	20
Span, ft	5.0
Rudder (hinge line perpendicular to fuselage center line):	
Chord, ft	1.25
Span, ft	5.0
Horizontal Tail:	
Sweepback (leading edge), deg	0
Airfoil section	NACA 0012
Aspect ratio	3.10
Chord, ft	3.0
Center section chord, ft	4.21
Area (including center body), sq ft	29.70
Span, ft	9.90
Dihedral	0

TABLE II.- WEIGHT OF THE FULL-SCALE AIRCRAFT WITH THE CENTER-OF-GRAVITY LOCATIONS FOR VARIOUS WING INCIDENCE ANGLES

[Weight, 3,139 lb]

i_w, deg	Center-of-gravity position (from wing pivot), ft	
	Horizontal (forward)	Vertical (below)
4	0.490	1.310
14	.477	1.250
20	.460	1.228
40	.394	1.120
60	.297	1.057
80	.180	1.023

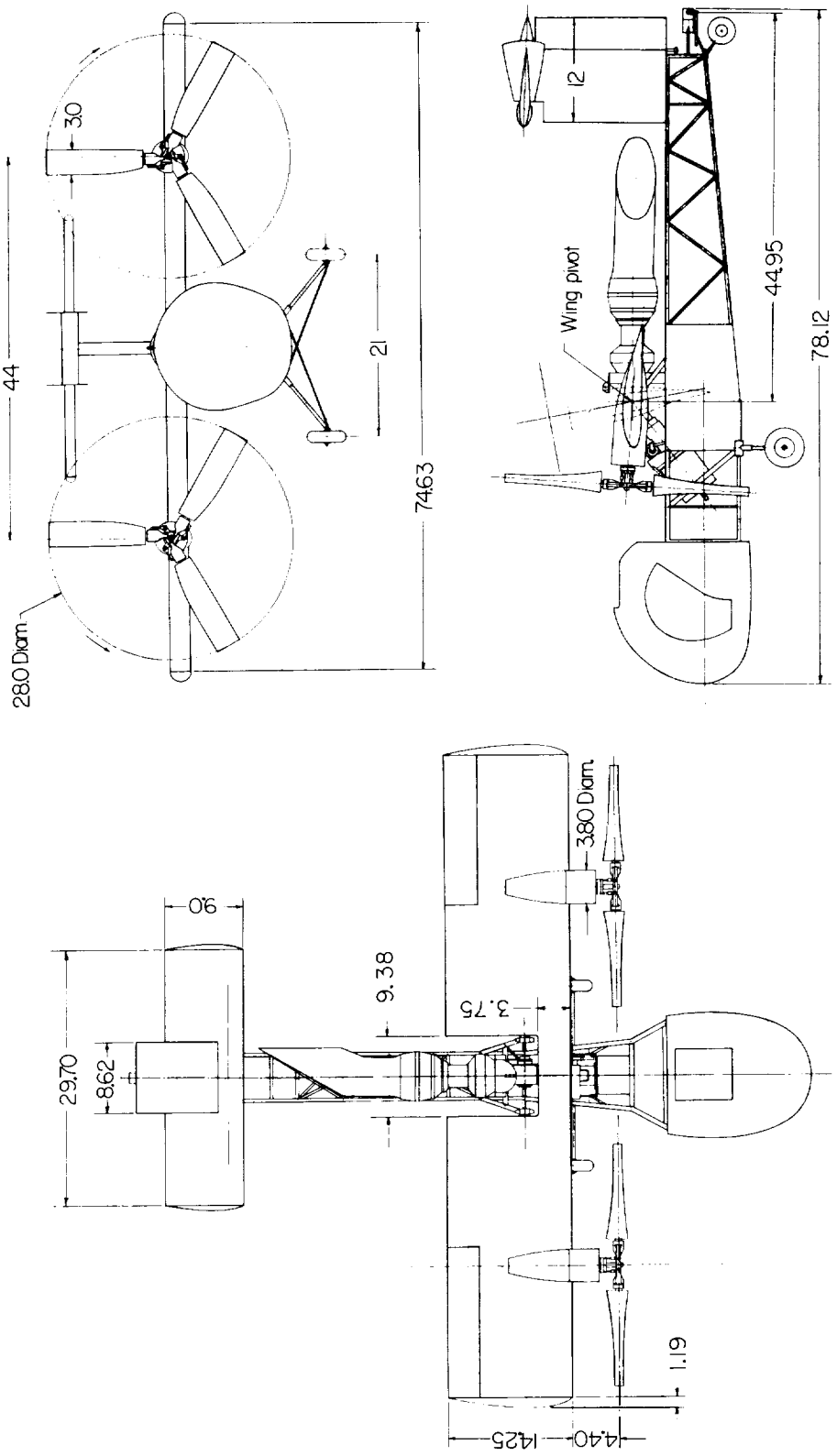

Figure 1.- Three-view sketch of model. All dimensions are in inches.

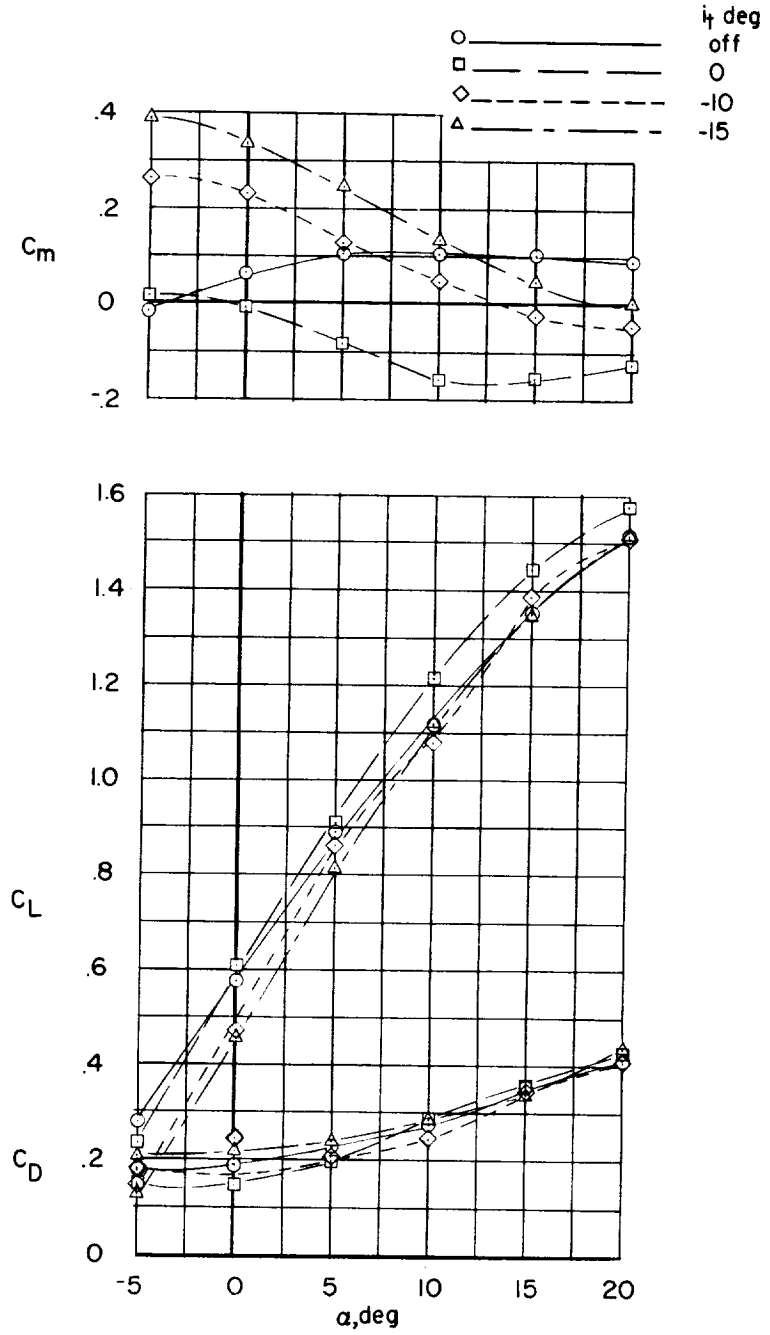

(a) $T_c' = 0$; $i_w = 4^\circ$.

Figure 2.- Longitudinal stability and control characteristics in normal forward flight.

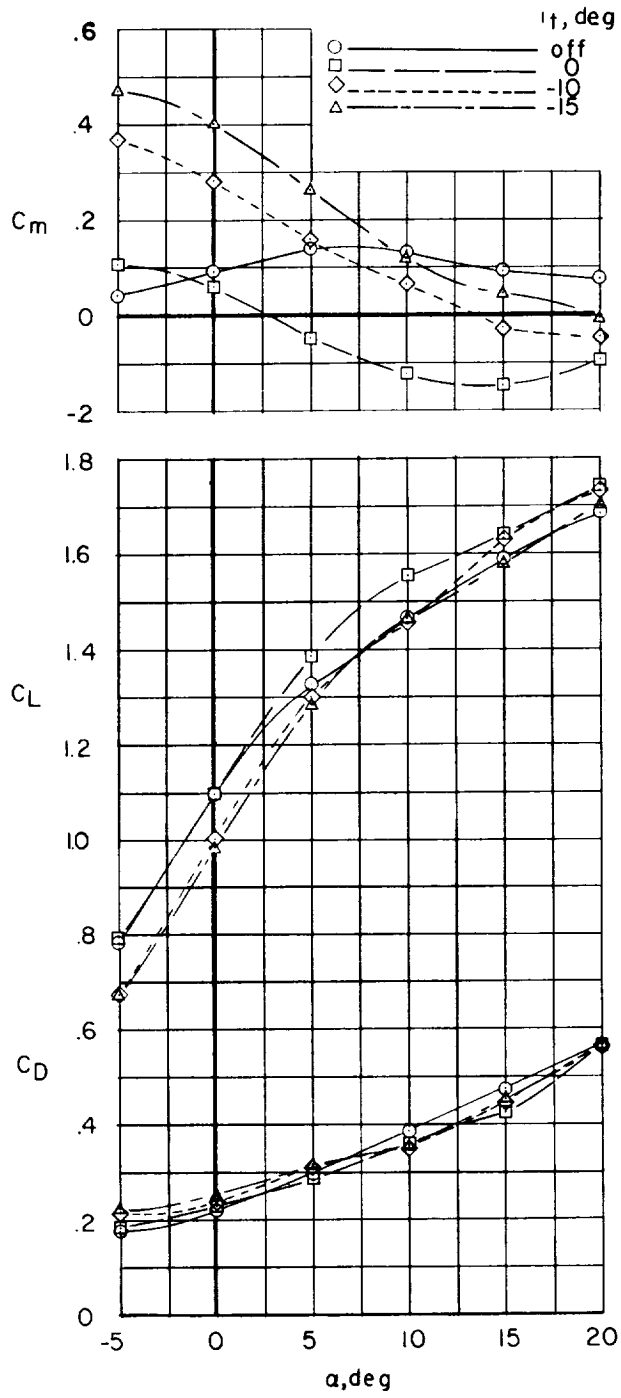

(b) $T_c' = 0$; $i_w = 14^\circ$.

Figure 2.- Continued.

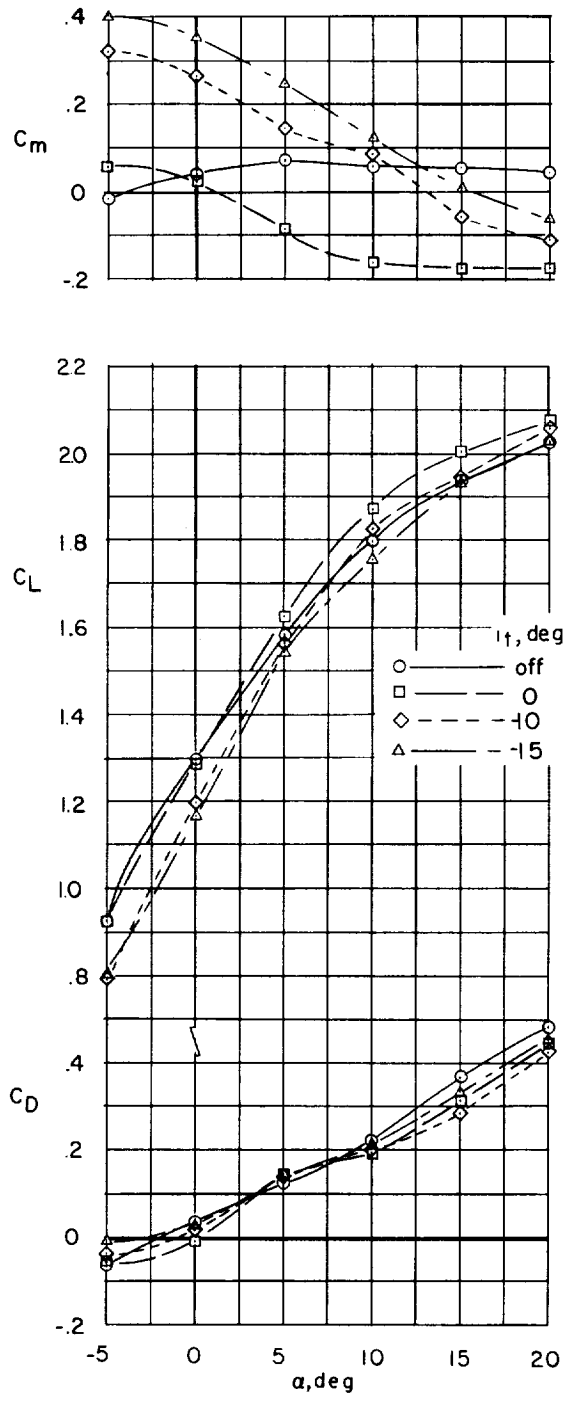

(c) $T_c' = 0.25$; $i_w = 4^\circ$.

Figure 2.- Continued.

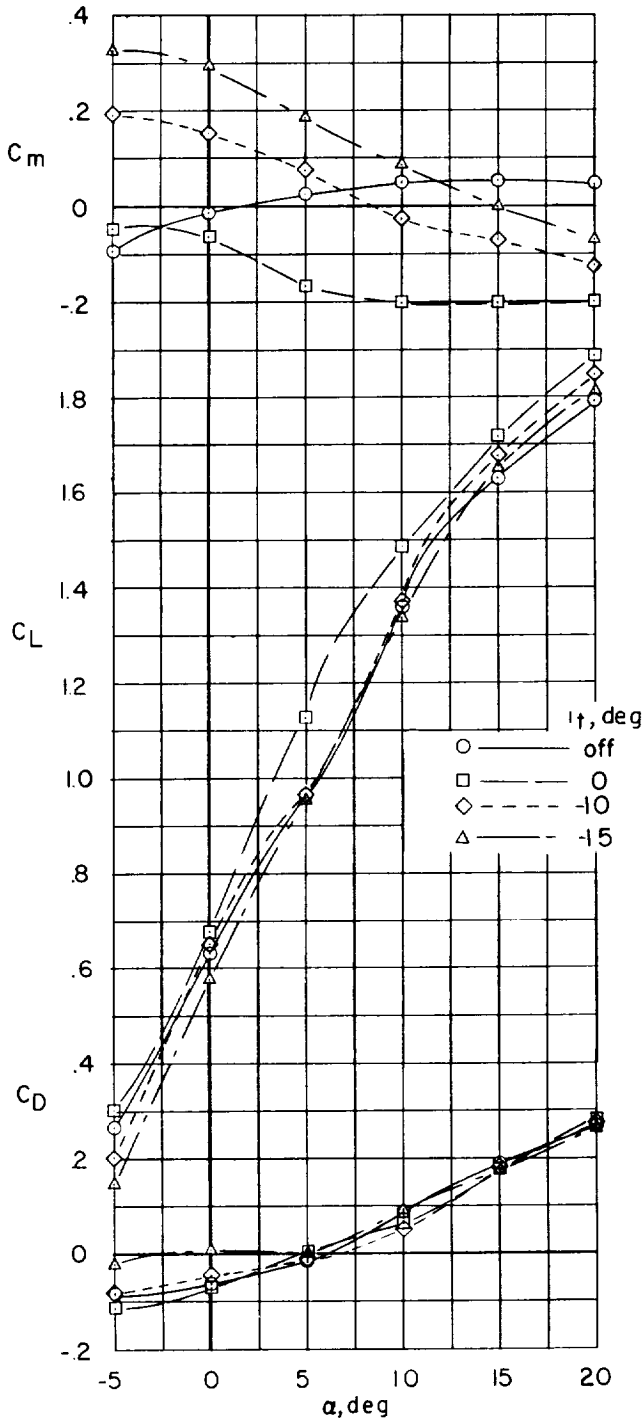

(d) $T_c' = 0.25$; $i_w = 14^o$.

Figure 2.- Continued.

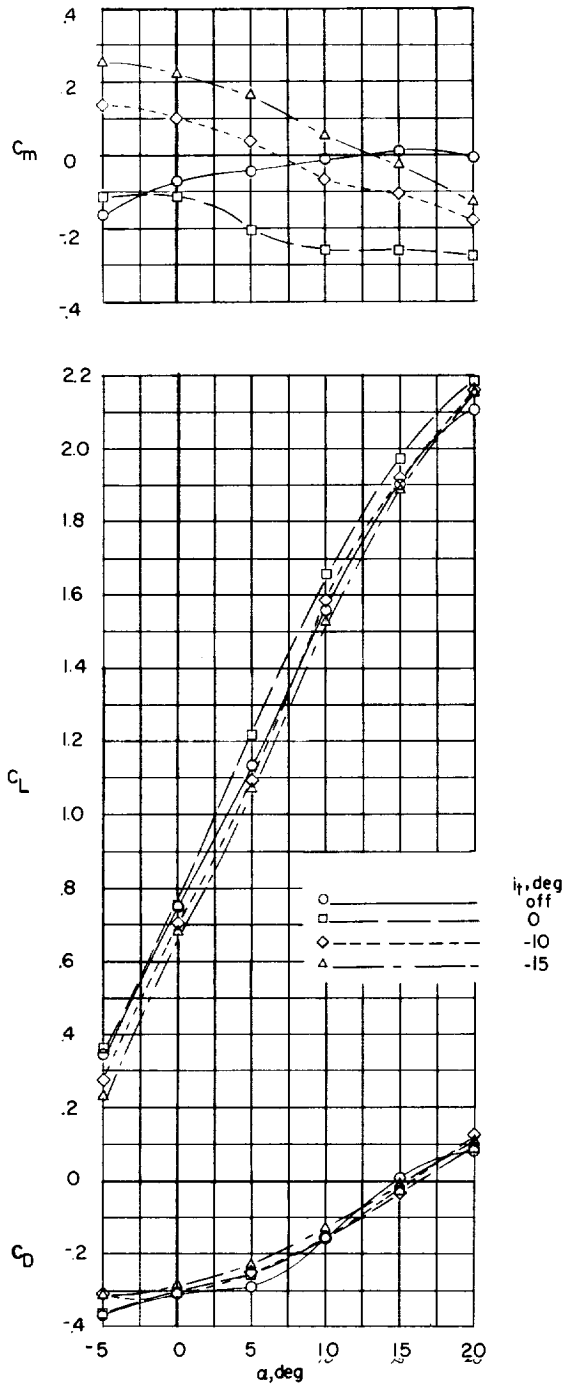

(e) $T_c' = 0.5$; $i_w = 4^\circ$.

Figure 2.- Concluded.

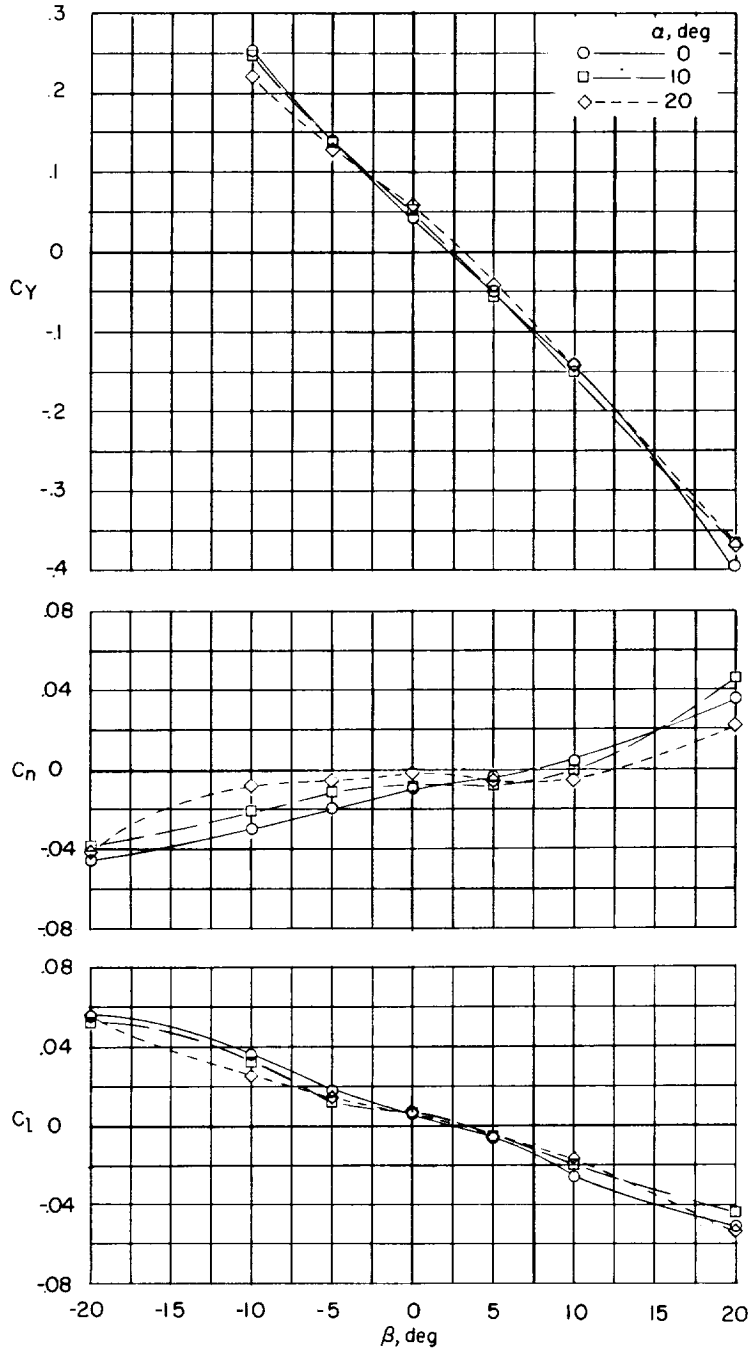

(a) $T_C' = 0$; $i_w = 4^\circ$.

Figure 3.- Lateral stability characteristics in normal forward flight.

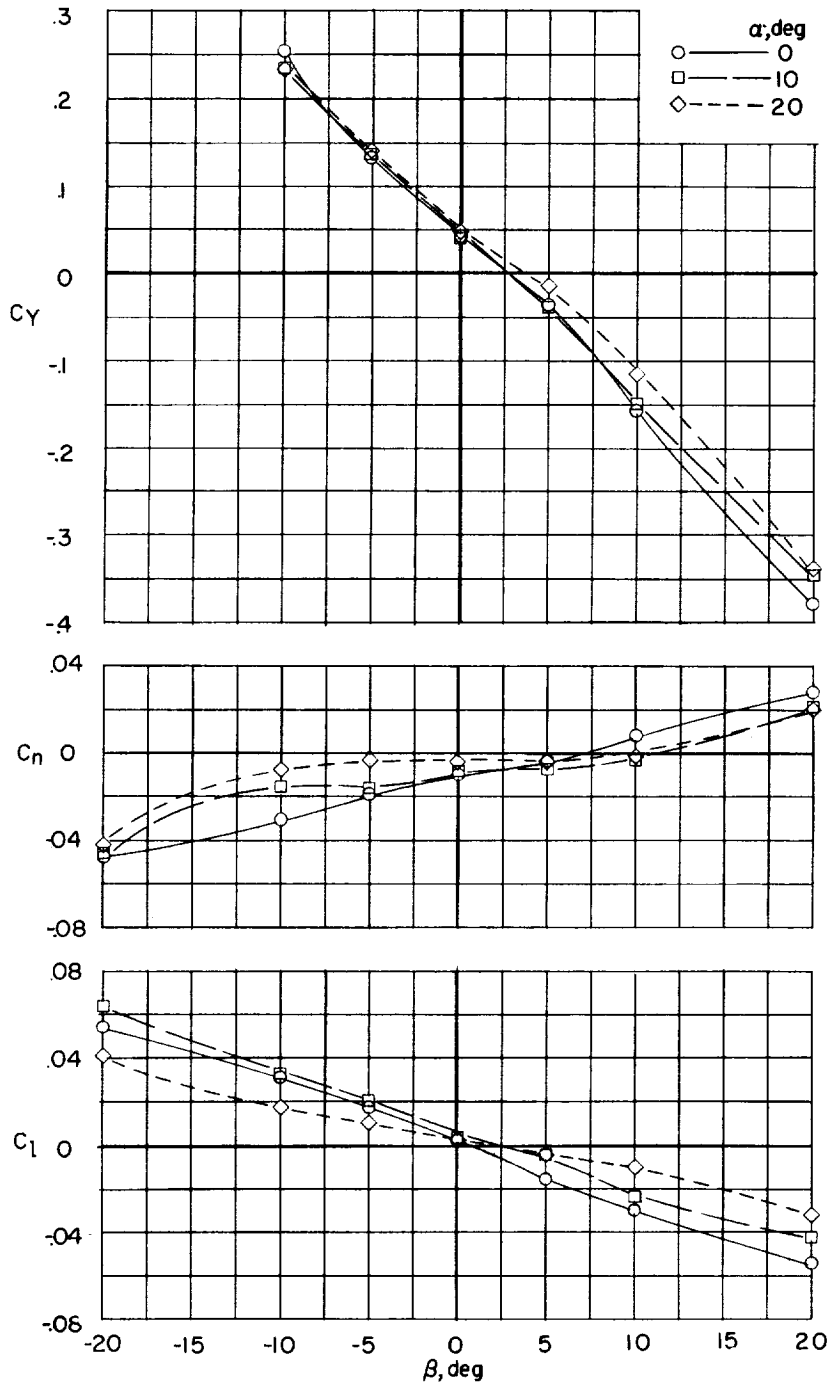

(b) $T_c' = 0$; $i_w = 14^\circ$.

Figure 3.- Continued.

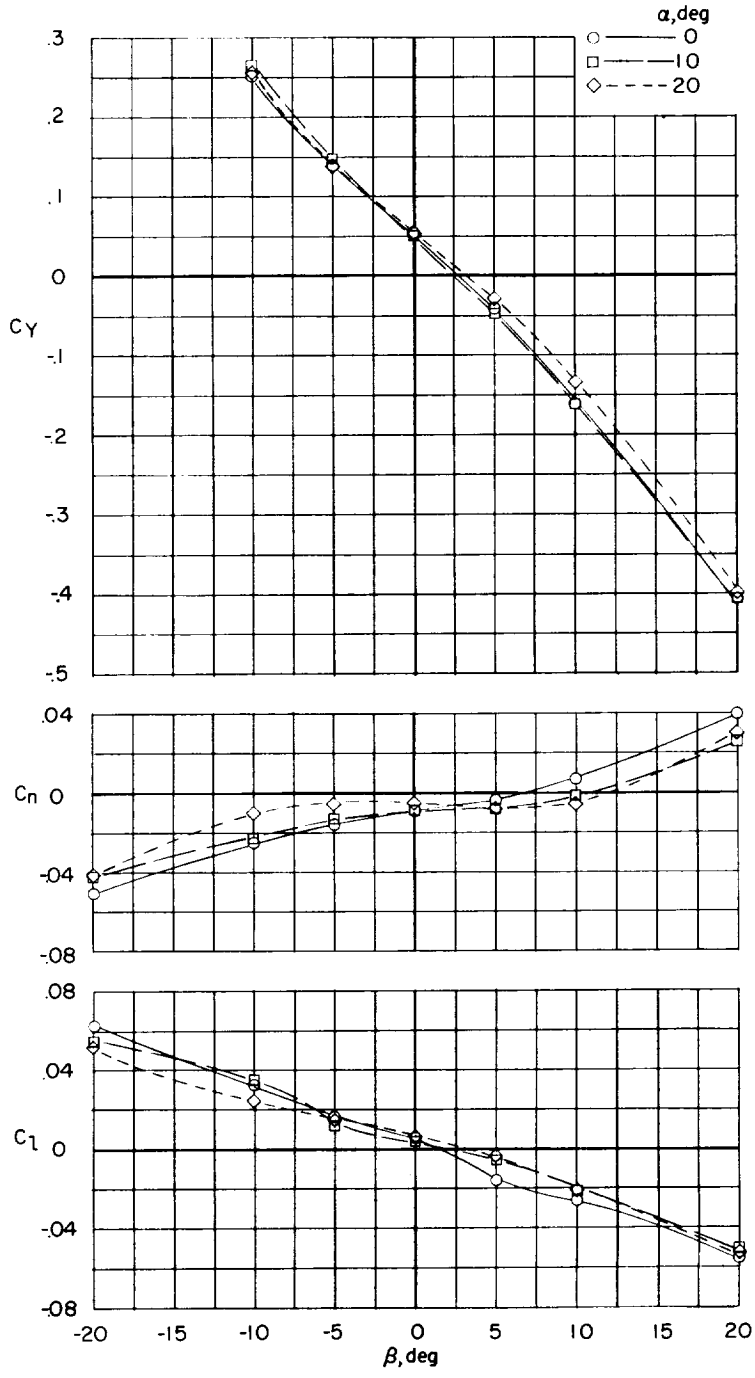

(c) $T_c' = 0.25$; $i_w = 4^\circ$.

Figure 3.- Continued.

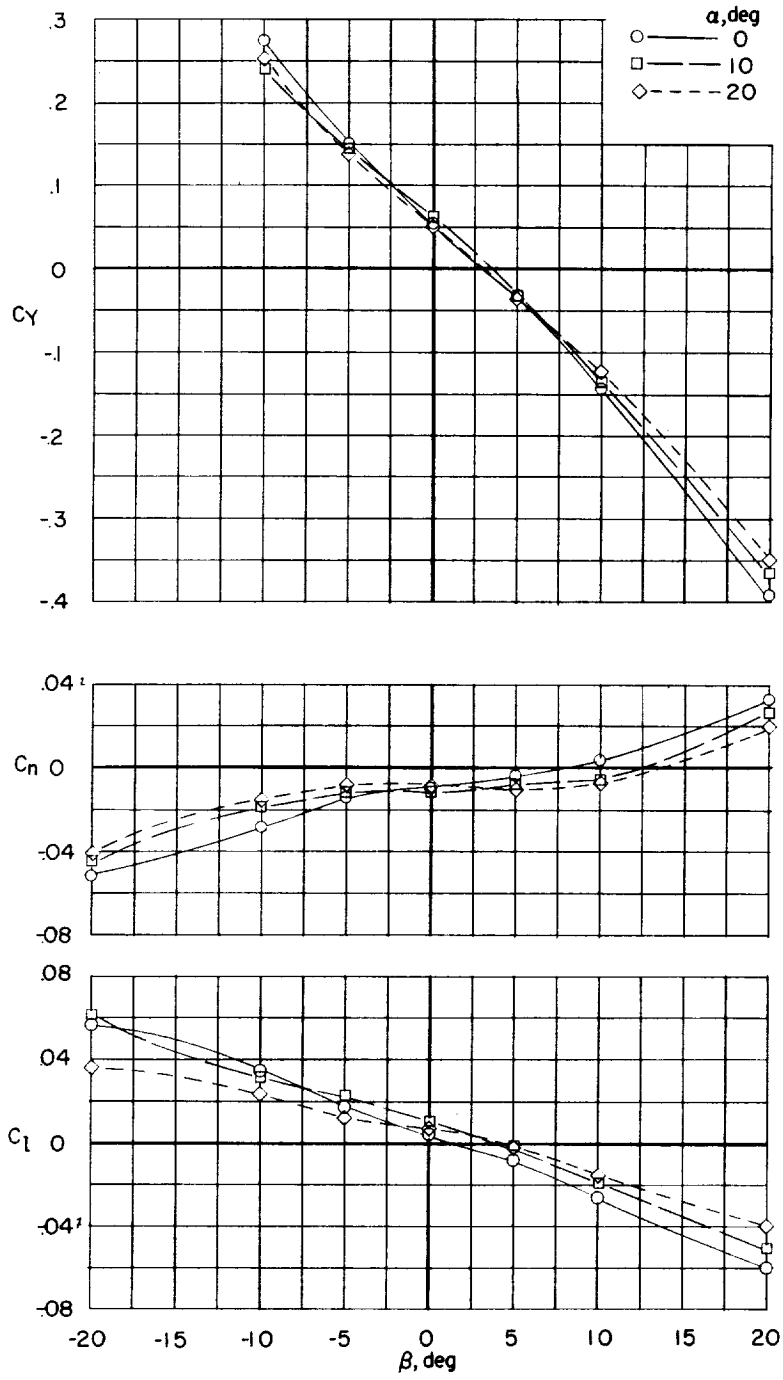

(d) $T_c' = 0.25$; $i_w = 14^o$.

Figure 3.- Continued.

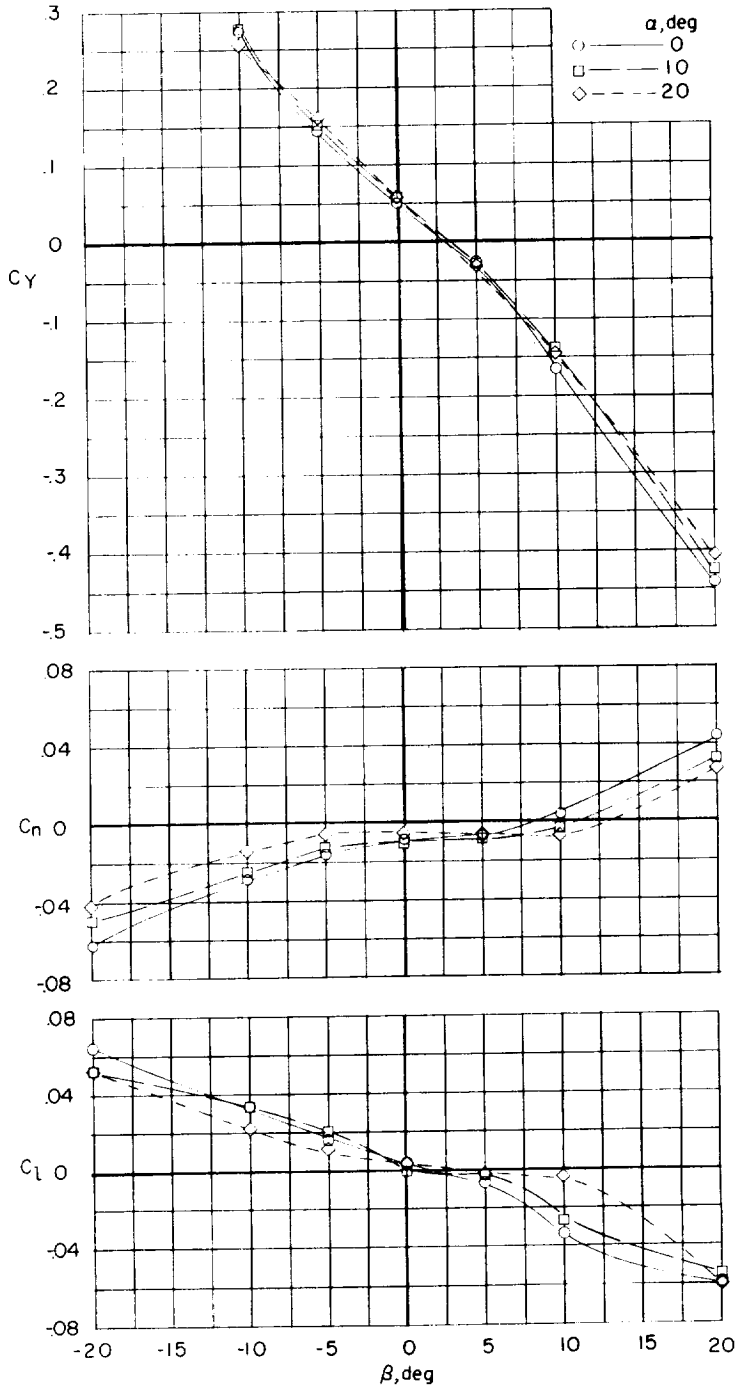

(e) $T_c' = 0.50$; $i_w = 4^o$.

Figure 3.- Concluded.

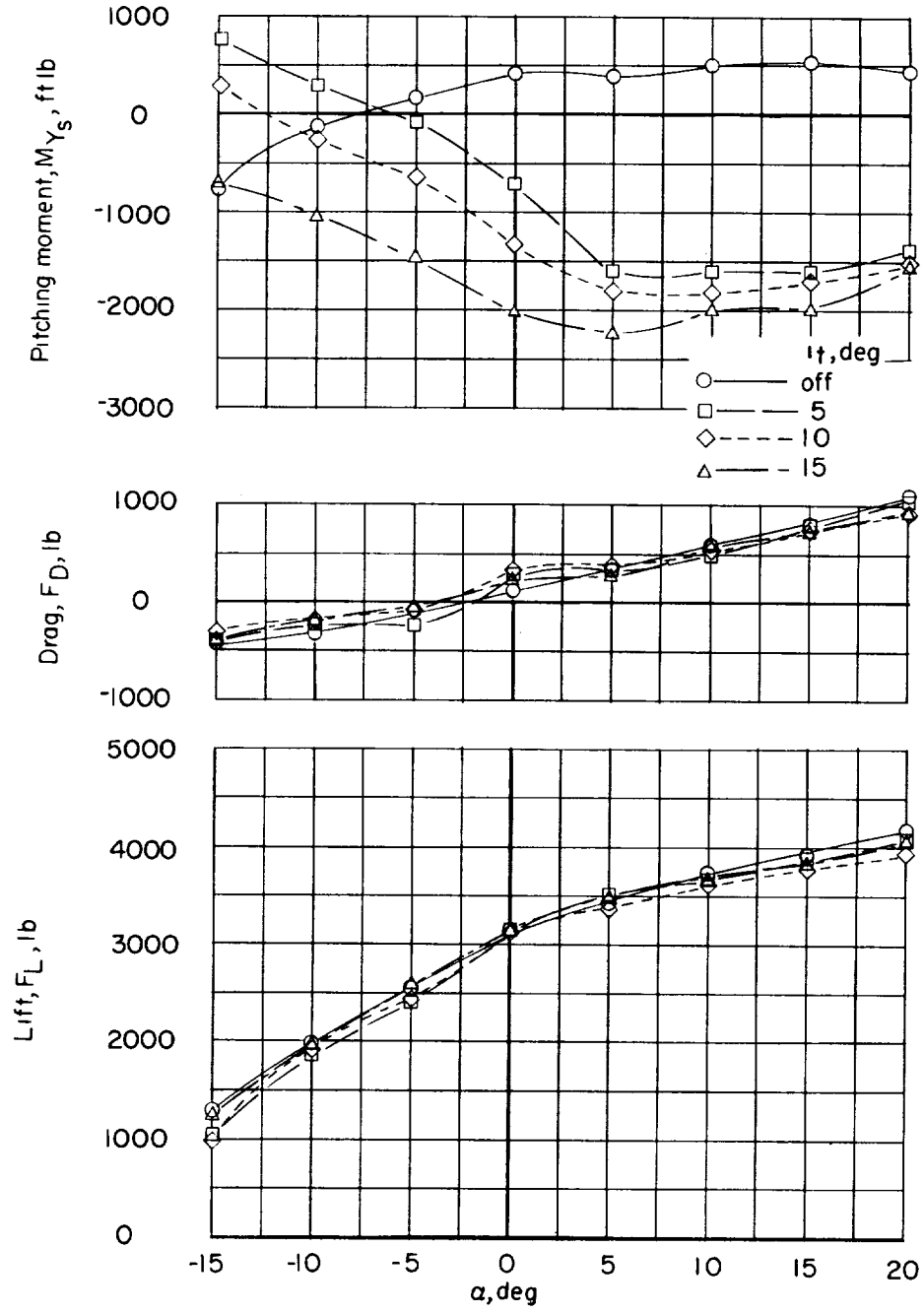

(a) $i_w = 20^\circ$; V = 68.5 knots.

Figure 4.- Longitudinal stability and control characteristics in the transition range with zero forward acceleration at $\alpha = 0$.

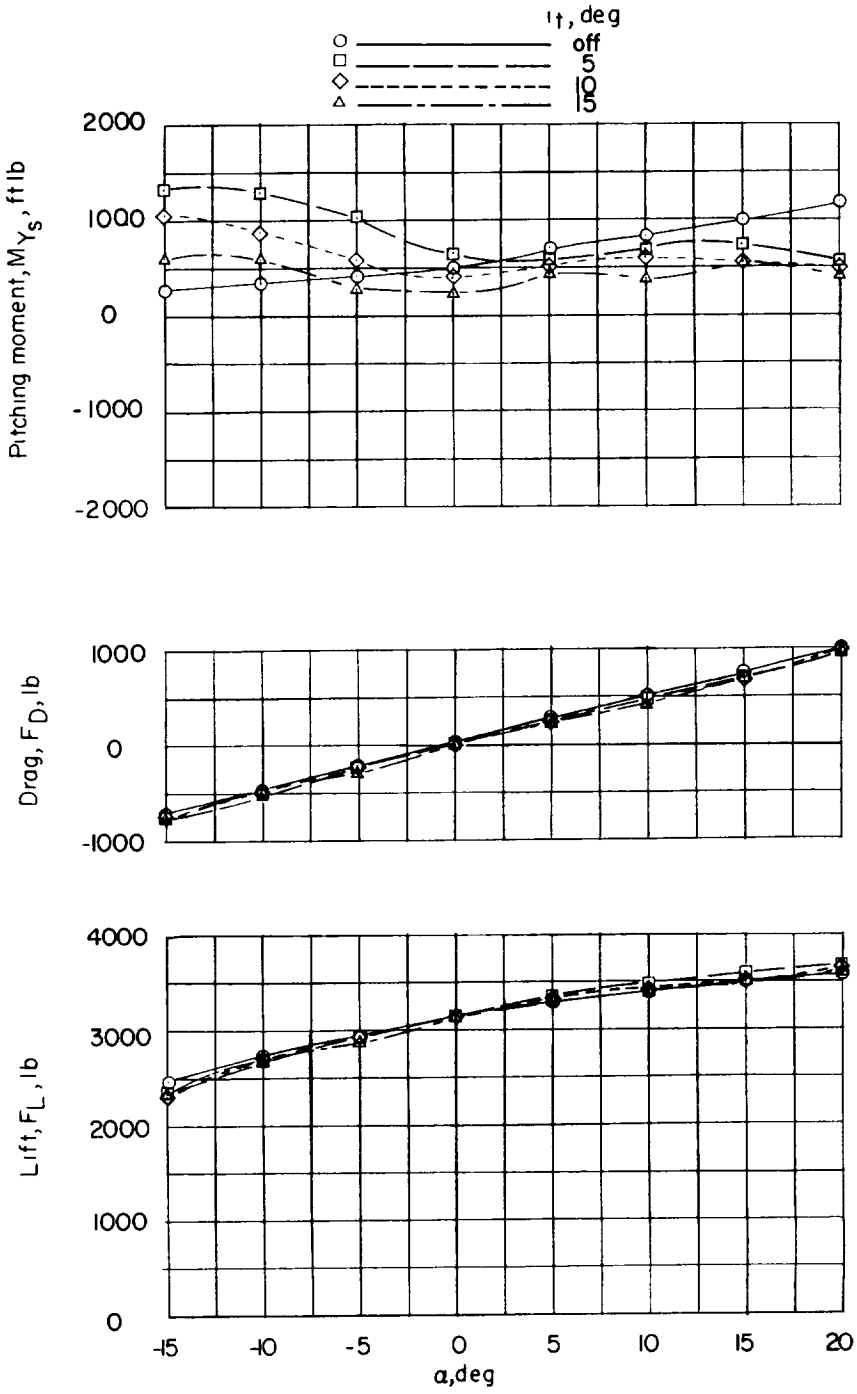

(b) $i_w = 40^o$; V = 43.0 knots.

Figure 4.- Continued.

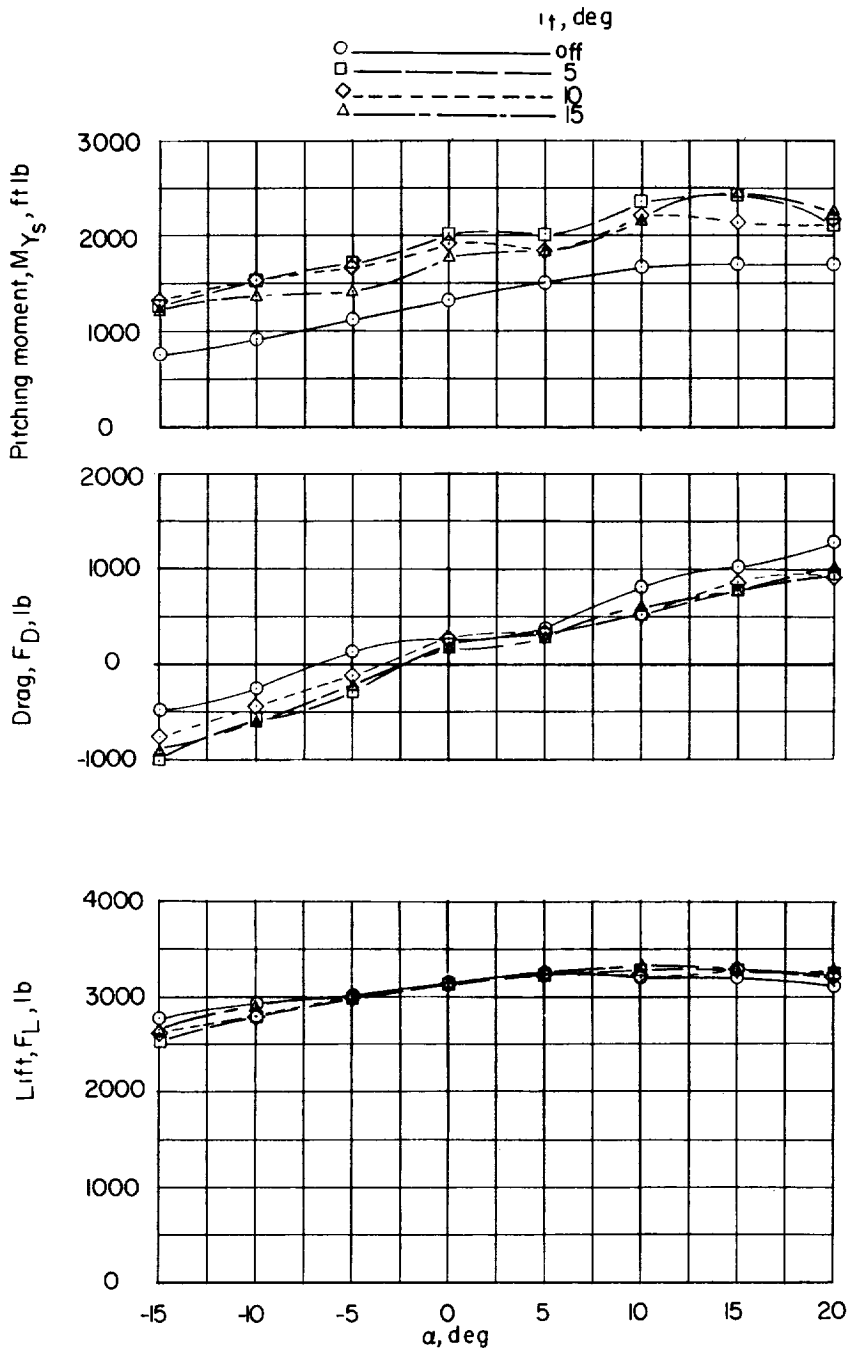

(c) $i_w = 60^\circ$; V = 29.8 knots.

Figure 4.- Continued.

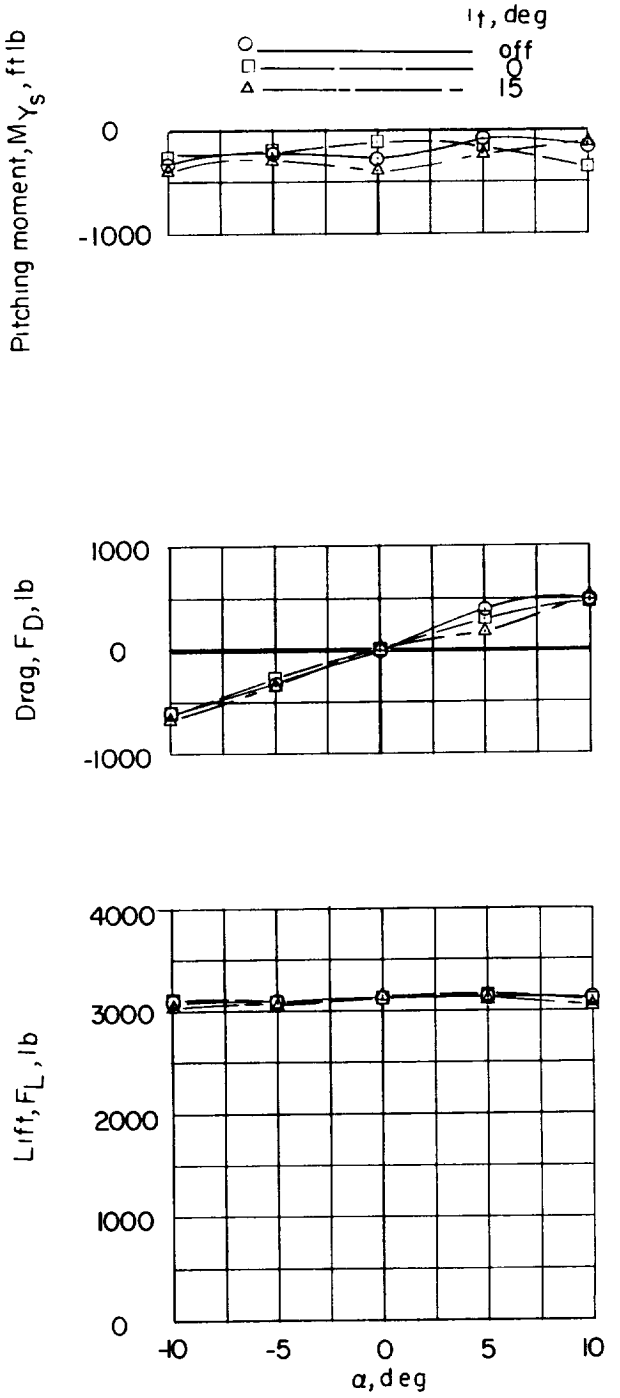

(d) $i_w = 80^\circ$; V = 8.53 knots.

Figure 4.- Concluded.

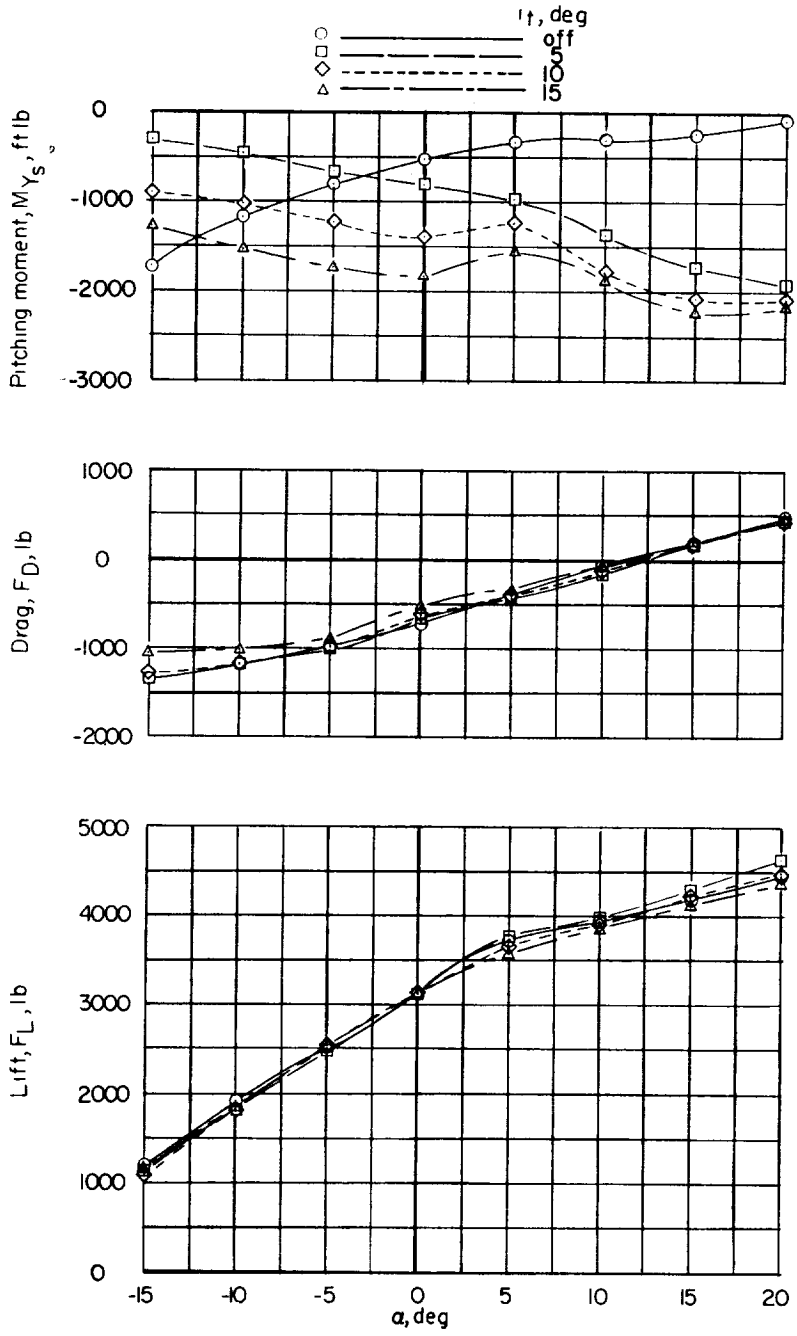

(a) $i_w = 20^\circ$; V = 57.8 knots.

Figure 5.- Longitudinal stability and control characteristics in the transition range with forward acceleration of 1/4g at $\alpha = 0^\circ$.

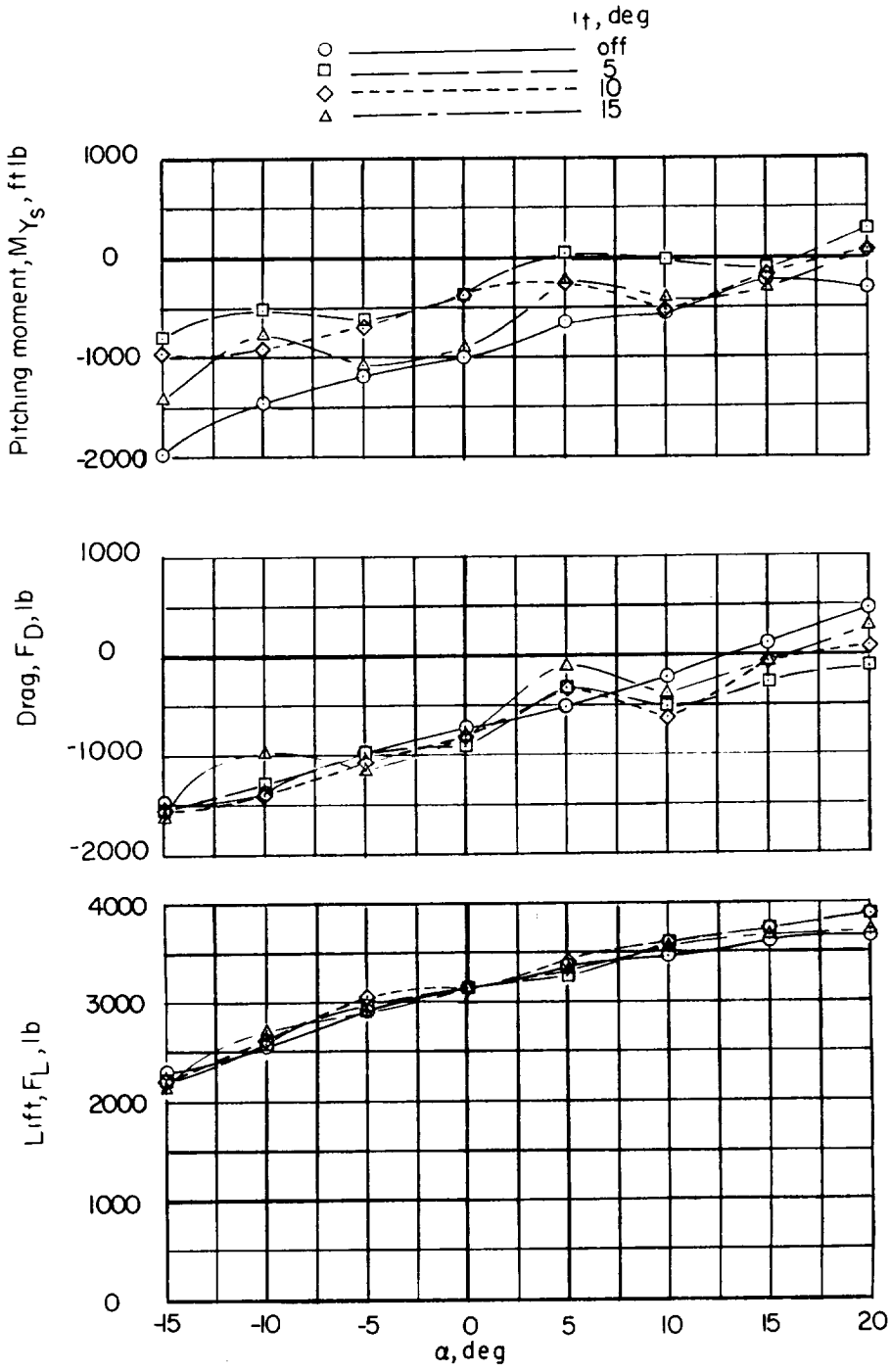

(b) $i_w = 40^\circ$; V = 35.9 knots.

Figure 5.- Continued.

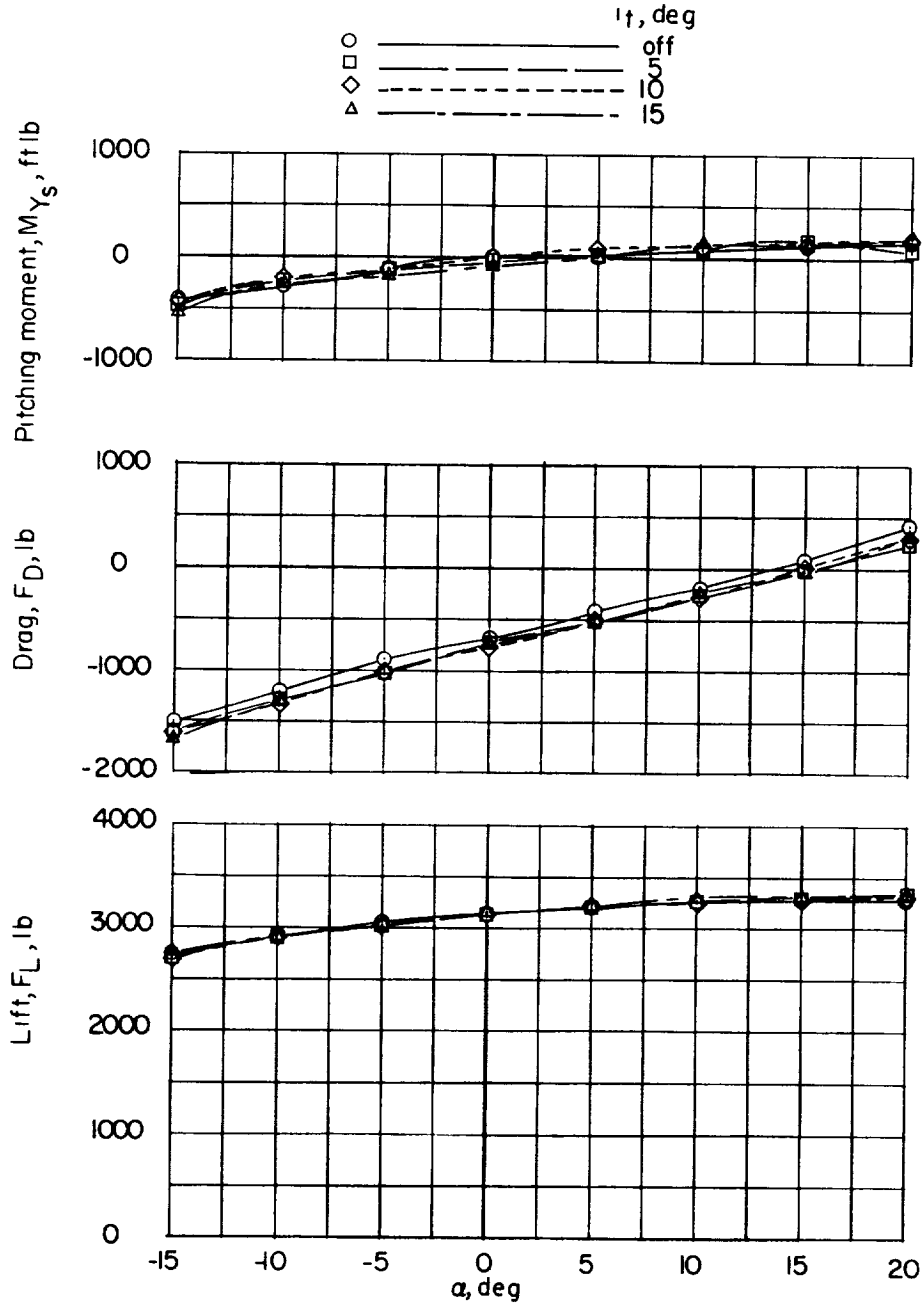

(c) $i_w = 60^\circ$; V = 14.5 knots.

Figure 5.- Concluded.

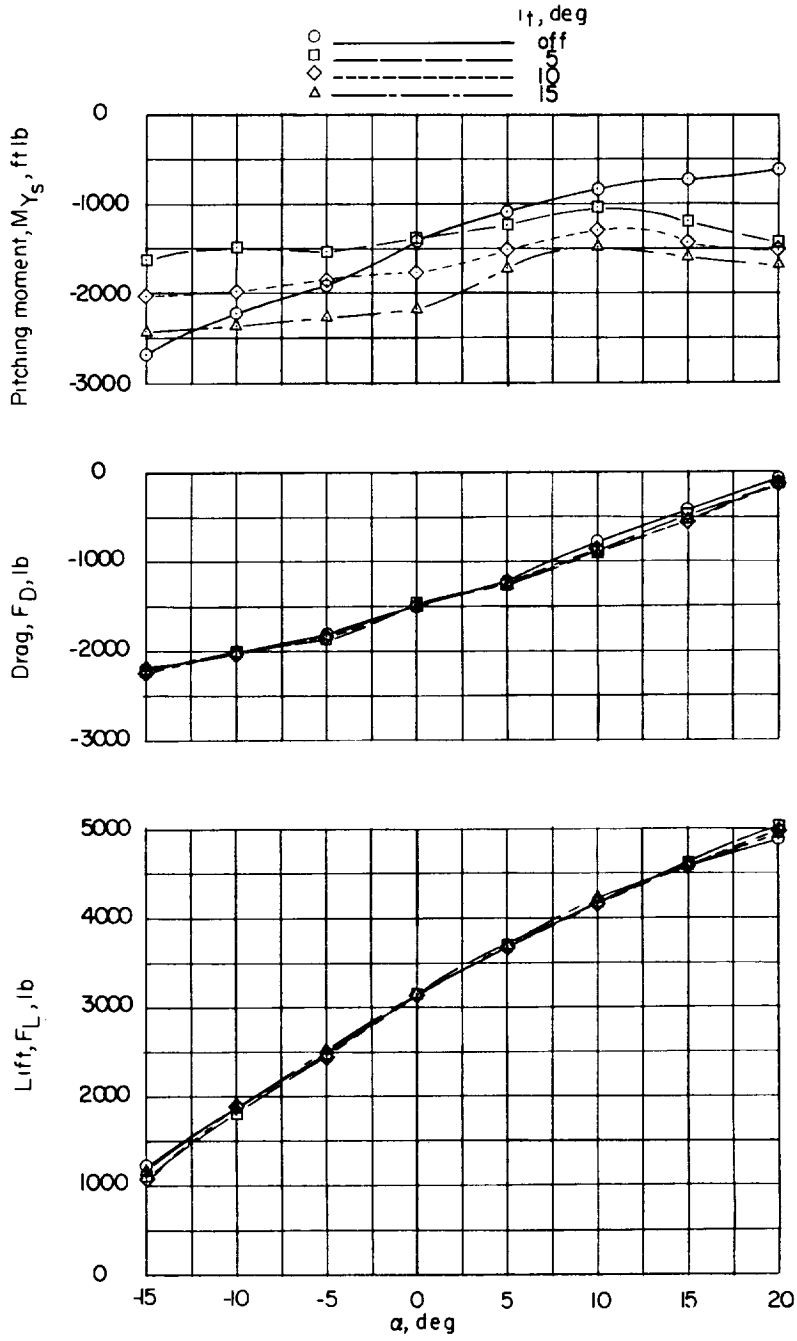

(a) $i_w = 20^\circ$; V = 49.5 knots.

Figure 6.- Longitudinal stability and control characteristics in the transition range with forward acceleration of 1/2g at $\alpha = 0^\circ$.

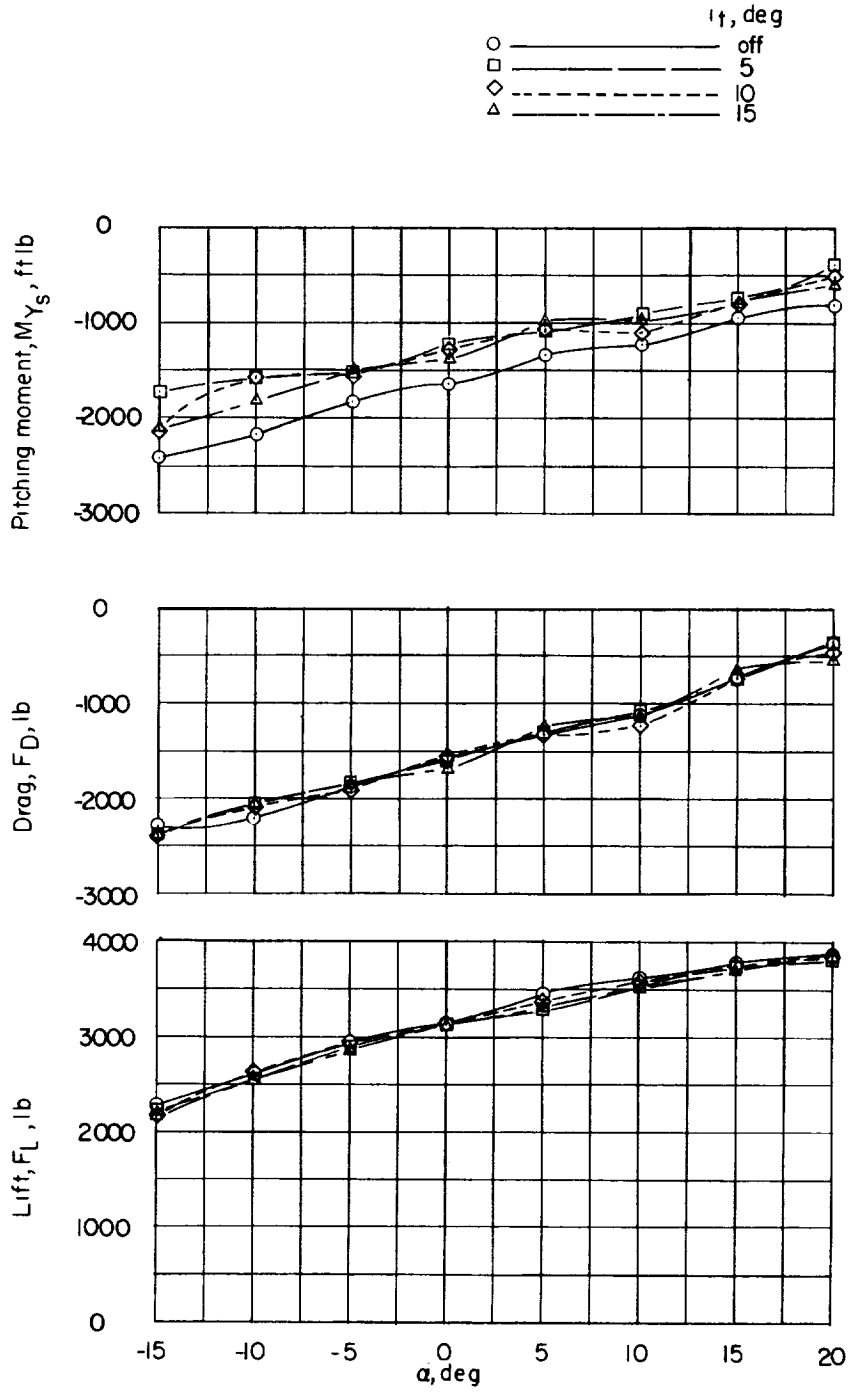

(b) $i_w = 40^\circ$; V = 25.1 knots.

Figure 6.- Concluded.

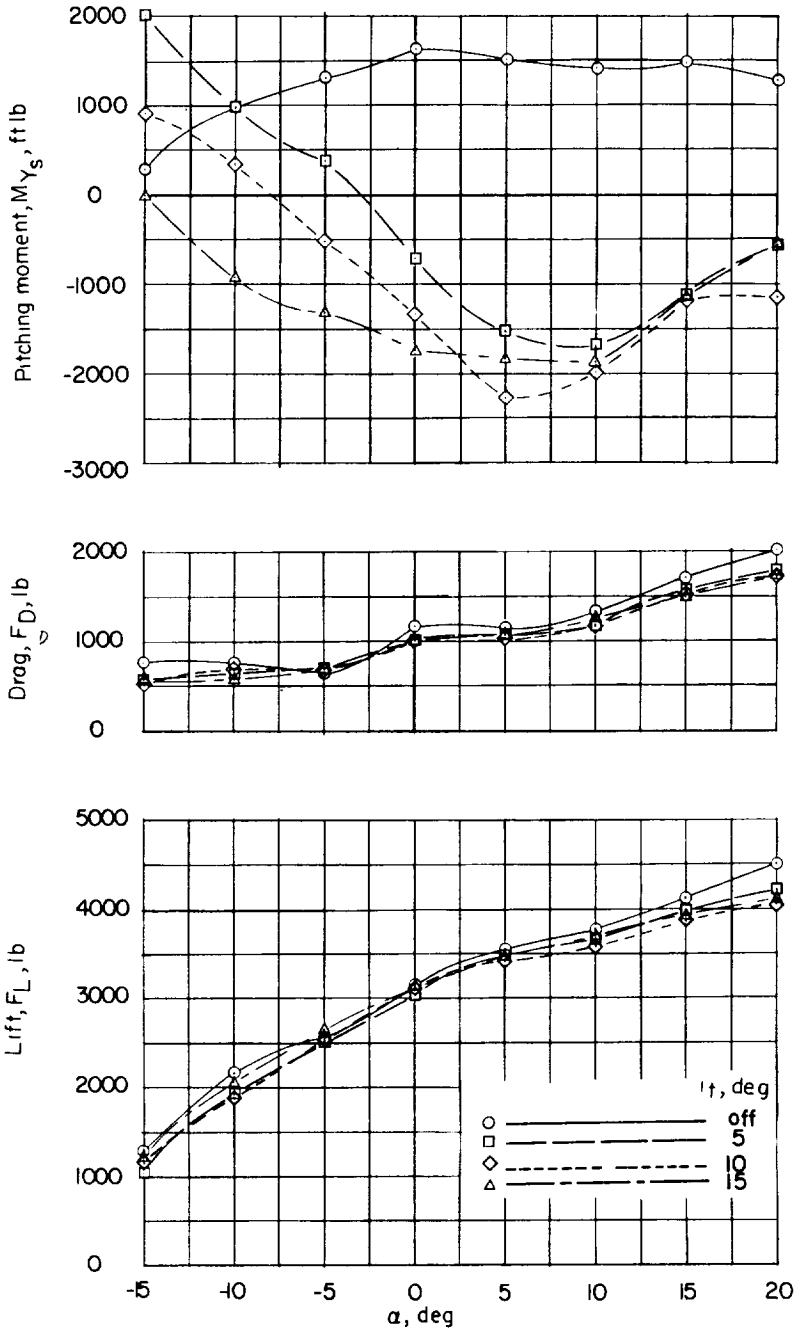

(a) $i_w = 20^\circ$; V = 82.5 knots.

Figure 7.- Longitudinal stability and control characteristics in the transition range with deceleration of 1/4g at $\alpha = 0^\circ$.

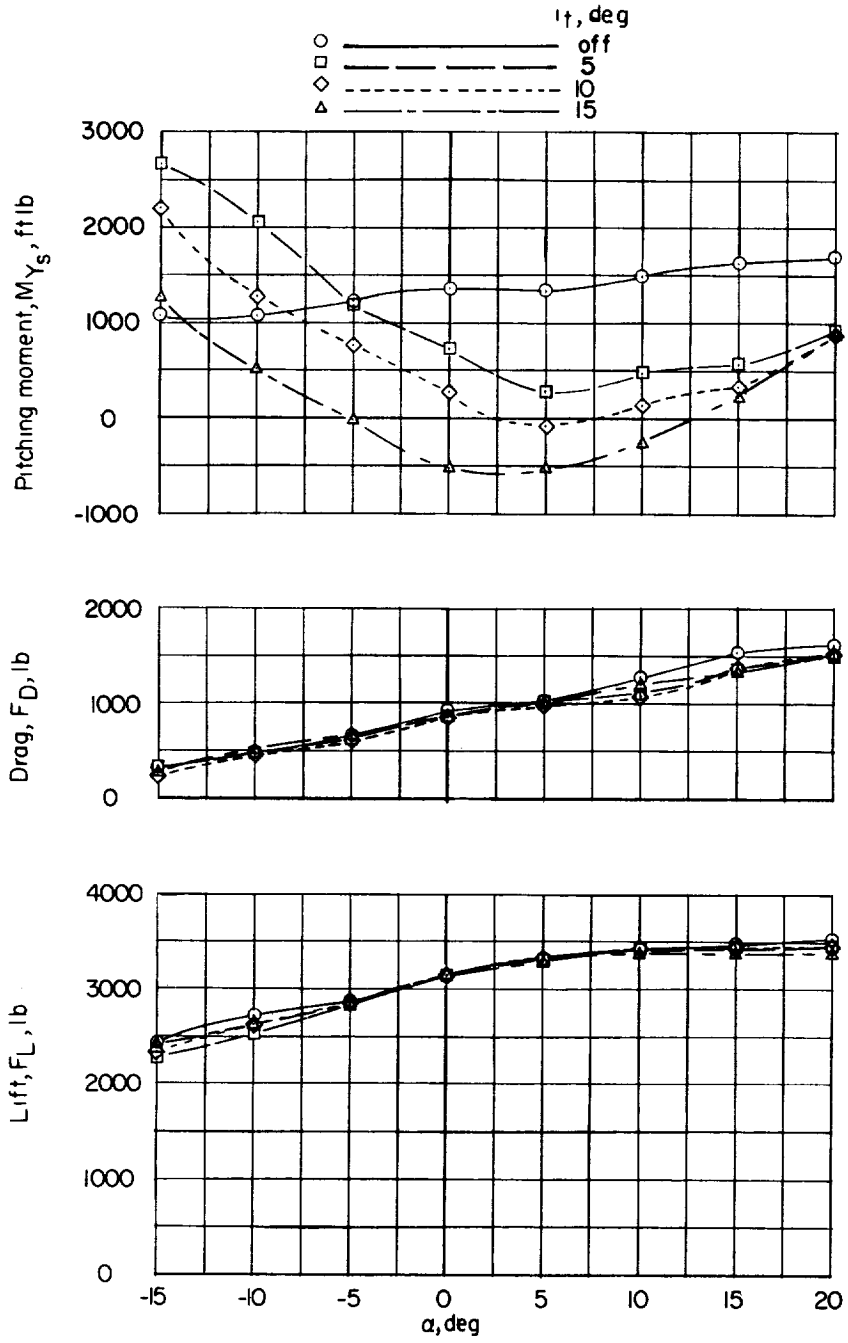

(b) $i_w = 40^\circ$; V = 63.7 knots.

Figure 7.- Continued.

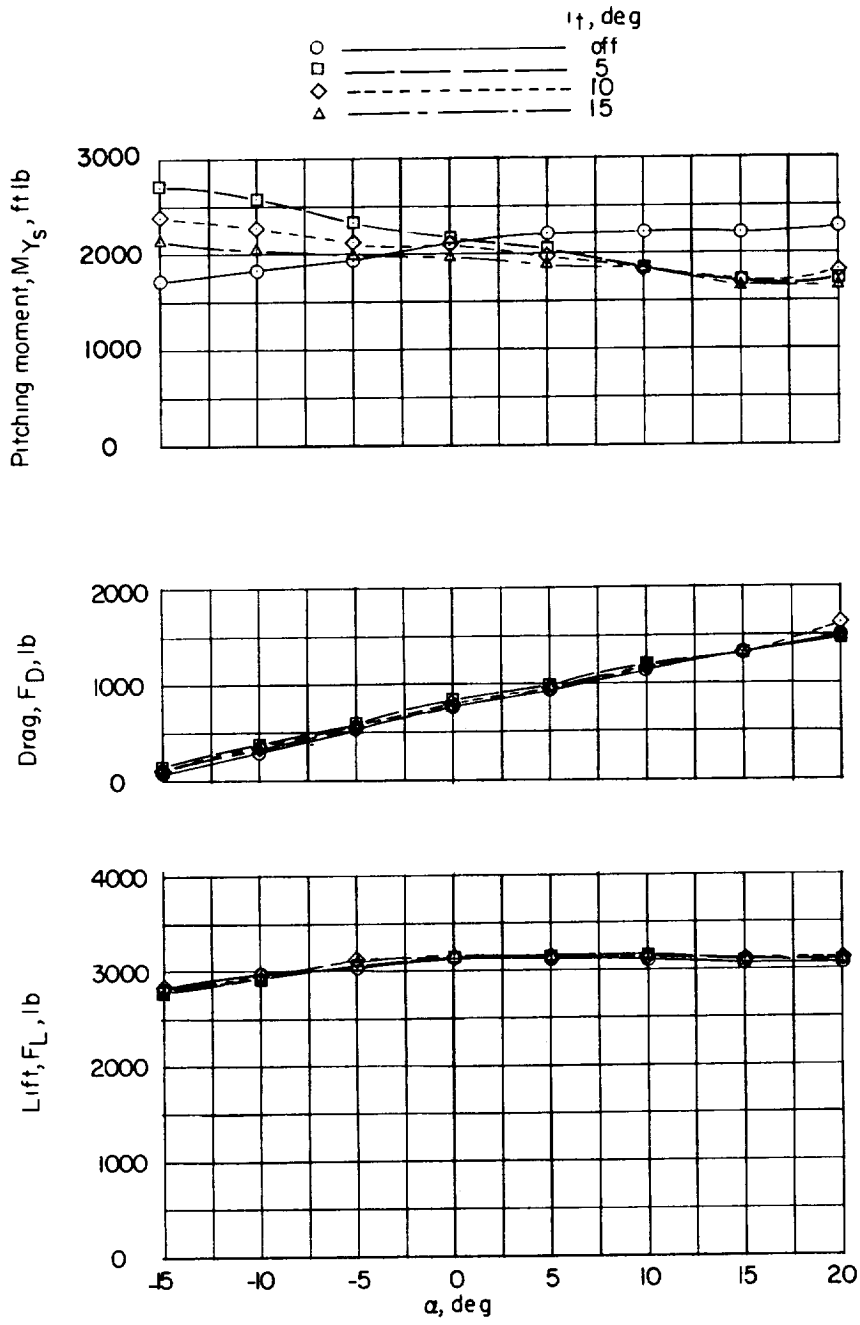

(c) $i_w = 60^\circ$; V = 38.9 knots.

Figure 7.- Concluded.

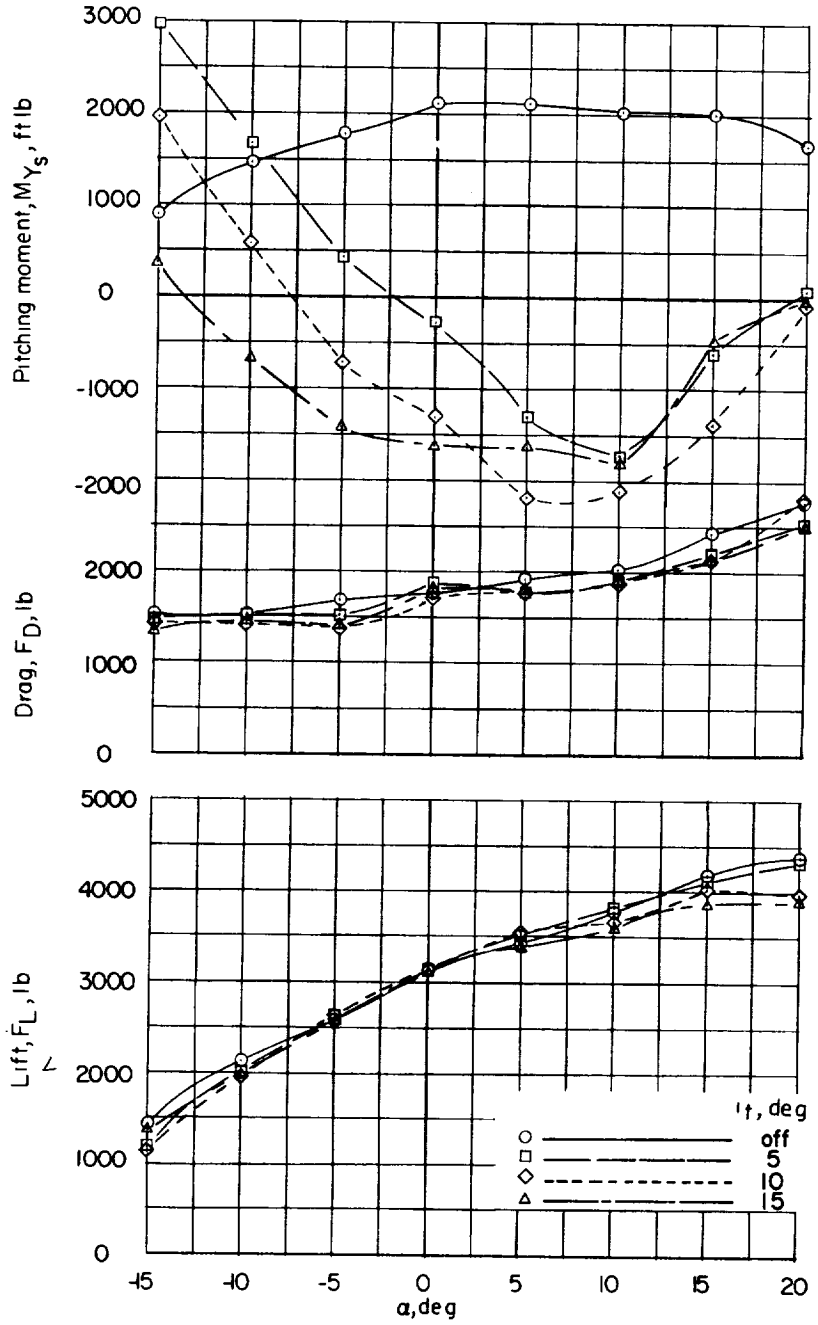

(a) $i_w = 20^\circ$; V = 103 knots.

Figure 8.- Longitudinal stability and control characteristics in the transition range with deceleration of 1/2g at $\alpha = 0^\circ$.

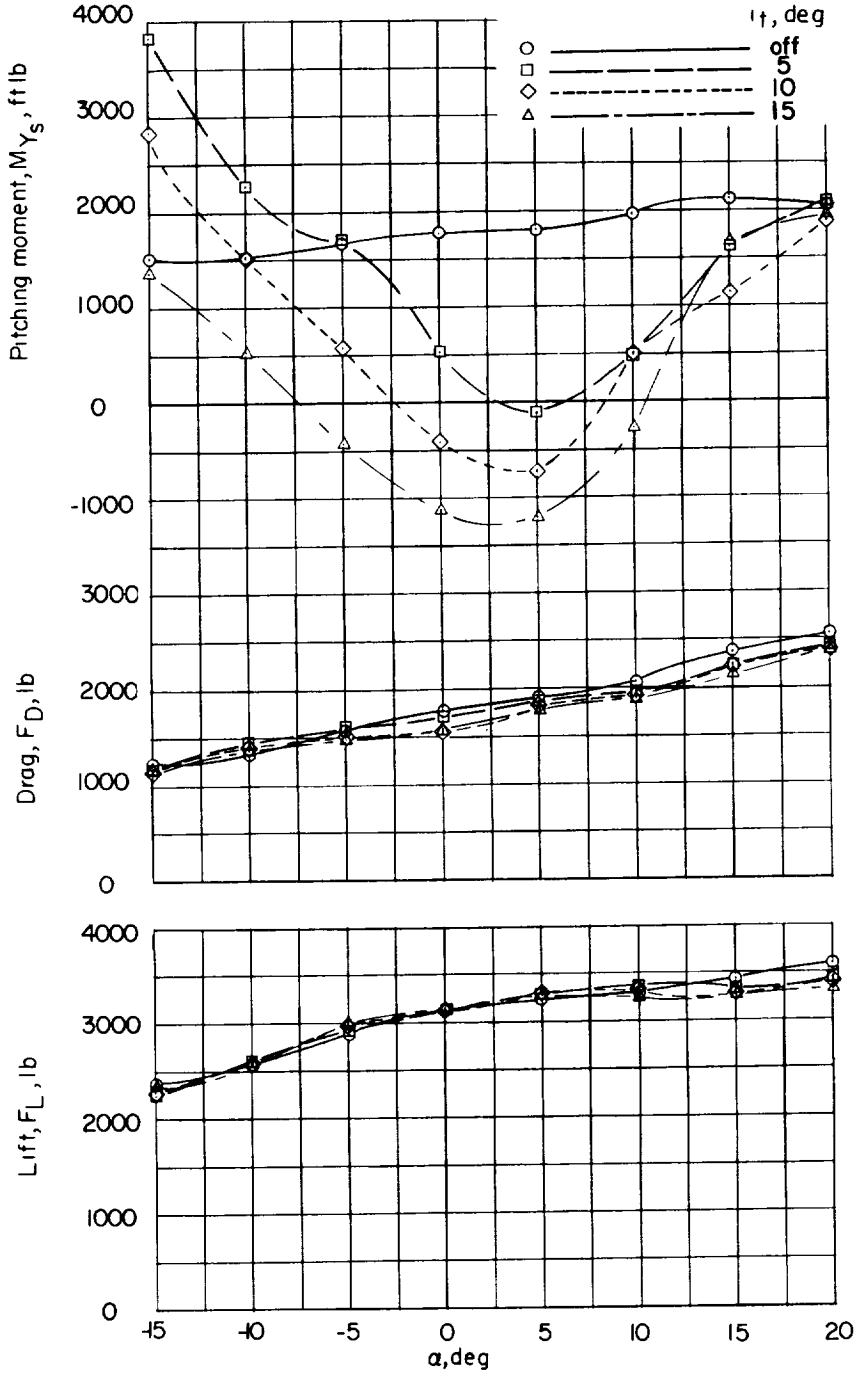

(b) $i_w = 40^\circ$; V = 241 knots.

Figure 8.- Continued.

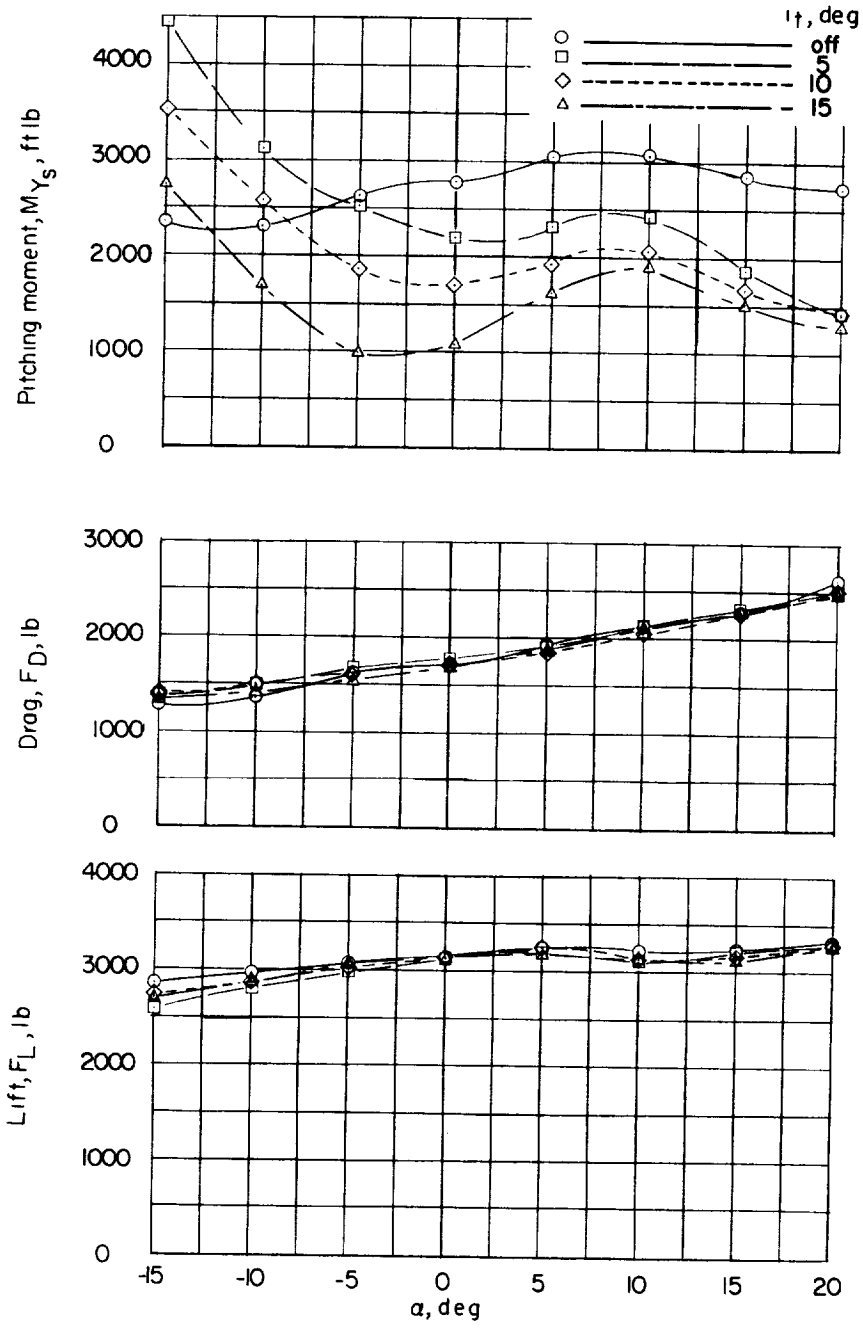

(c) $i_w = 60^\circ$; V = 66.8 knots.

Figure 8.- Concluded.

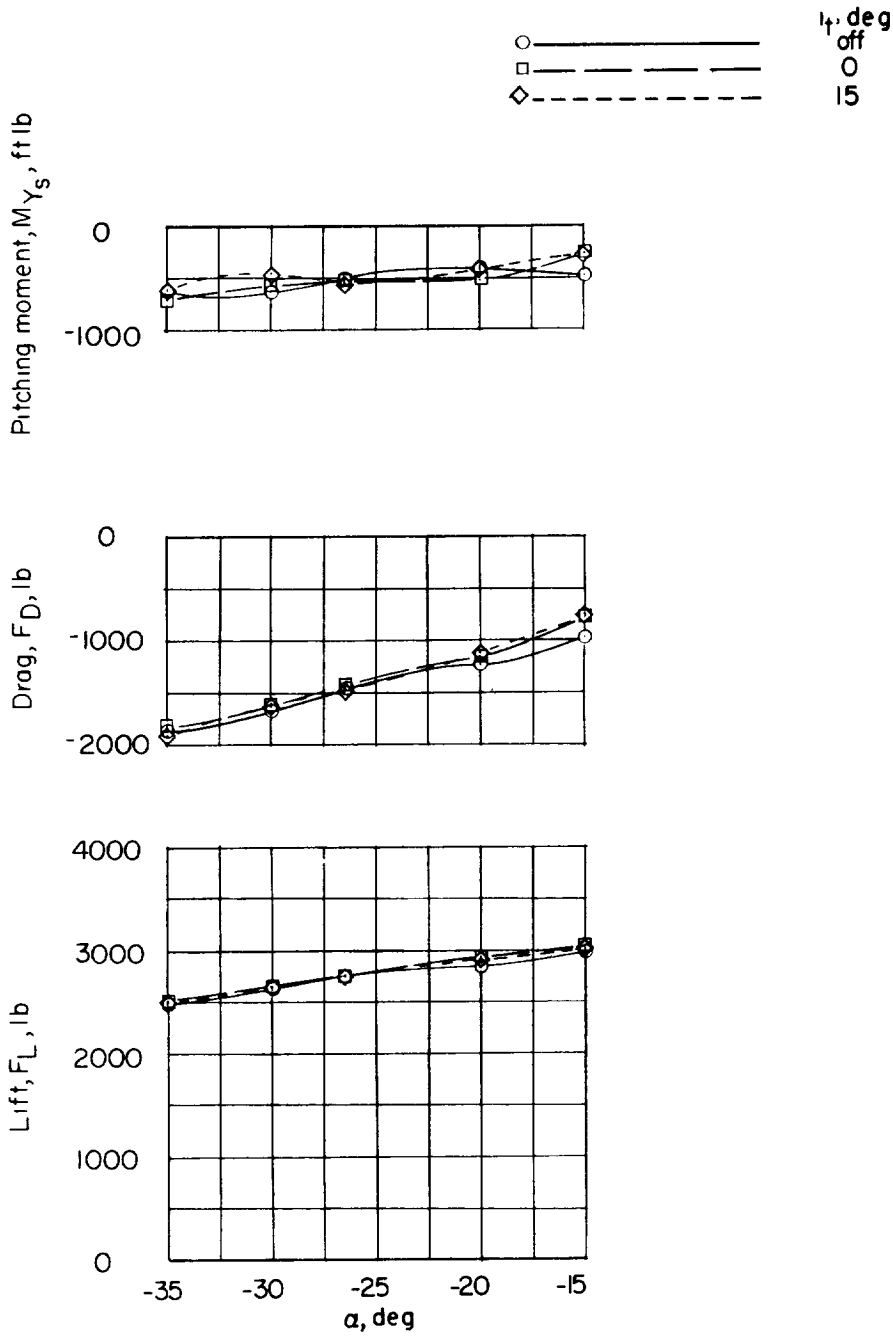

(a) 26.5° climb at $\alpha = -26.5^{\circ}$; V = 8.58 knots.

Figure 9.- Longitudinal stability and control characteristics in climb and descent conditions at $i_w = 80^{\circ}$.

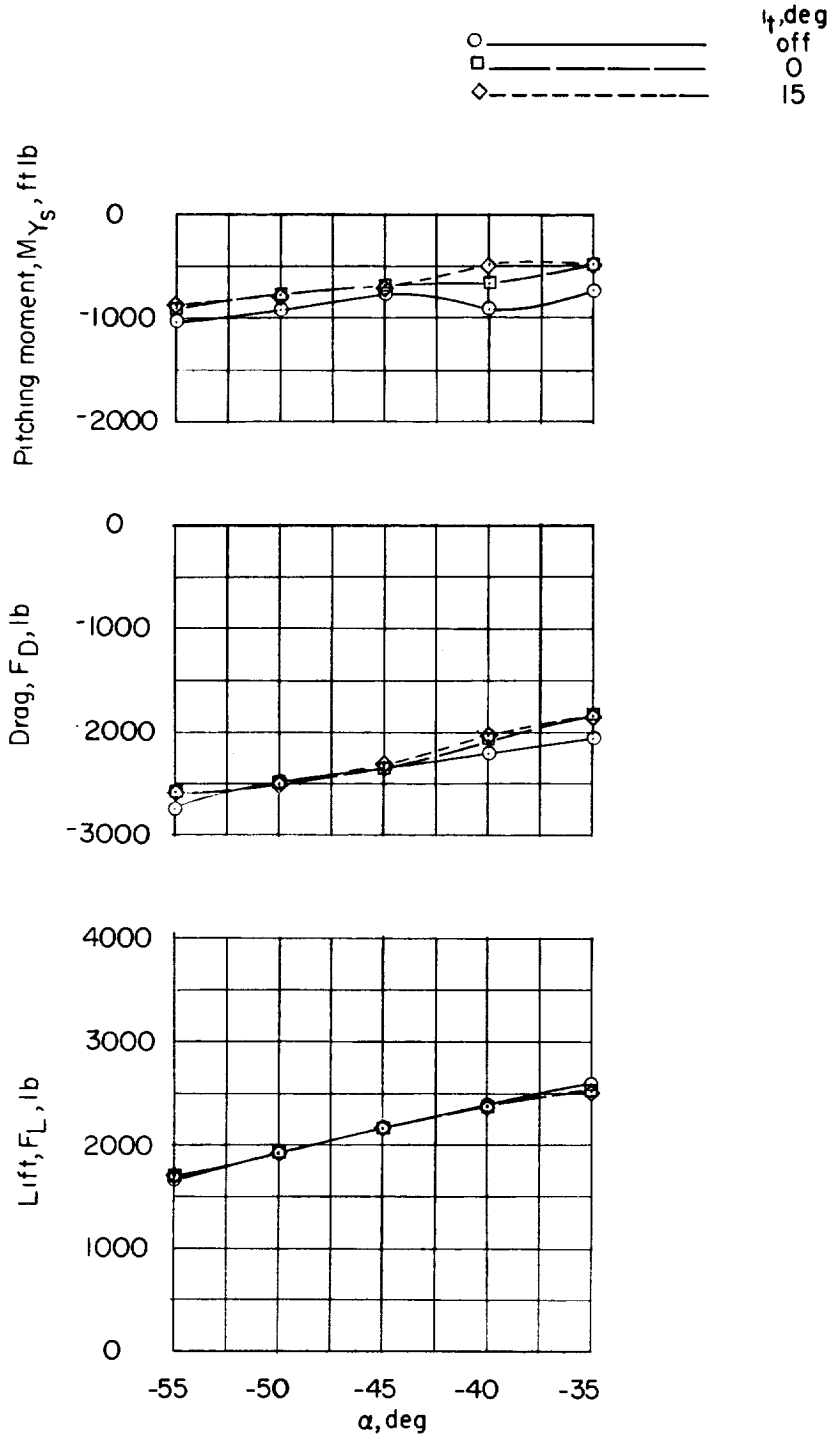

(b) 45° climb at $\alpha = -45^\circ$; V = 9.27 knots.

Figure 9.- Continued.

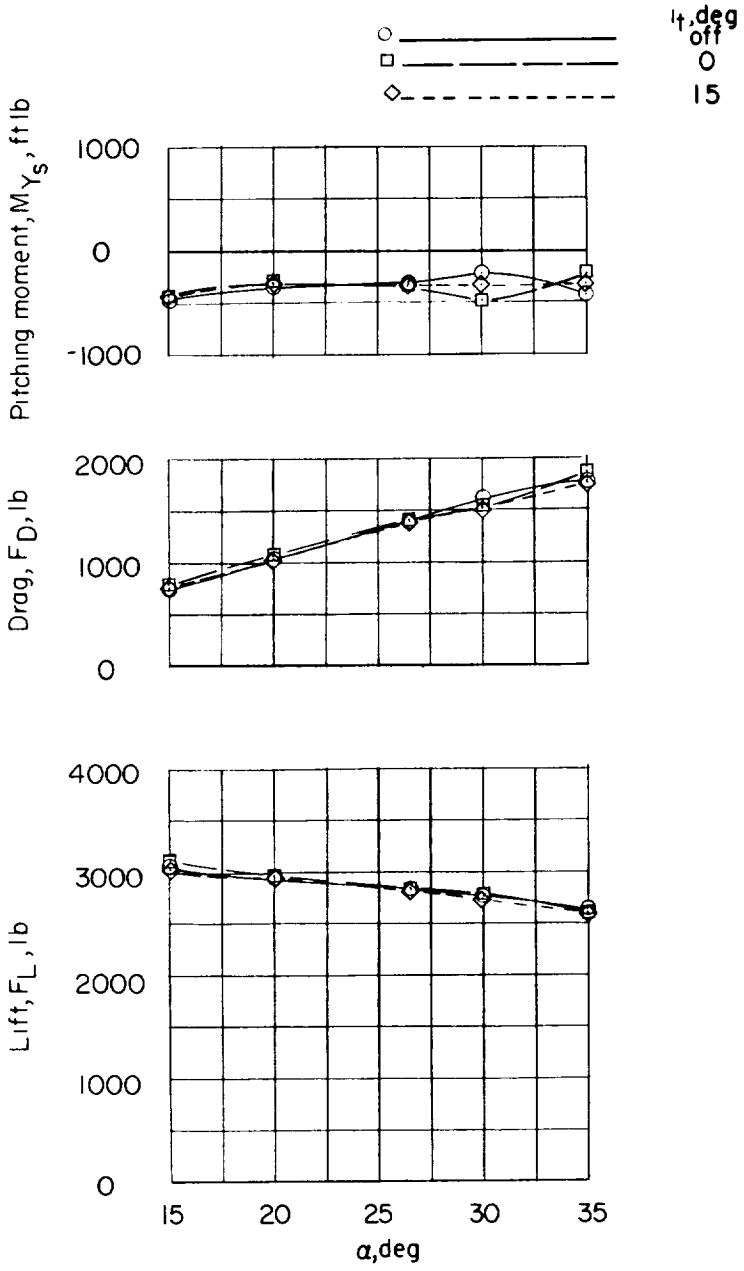

(c) 26.5° descent at α = 26.5°; V = 5.8 knots.

Figure 9.- Continued.

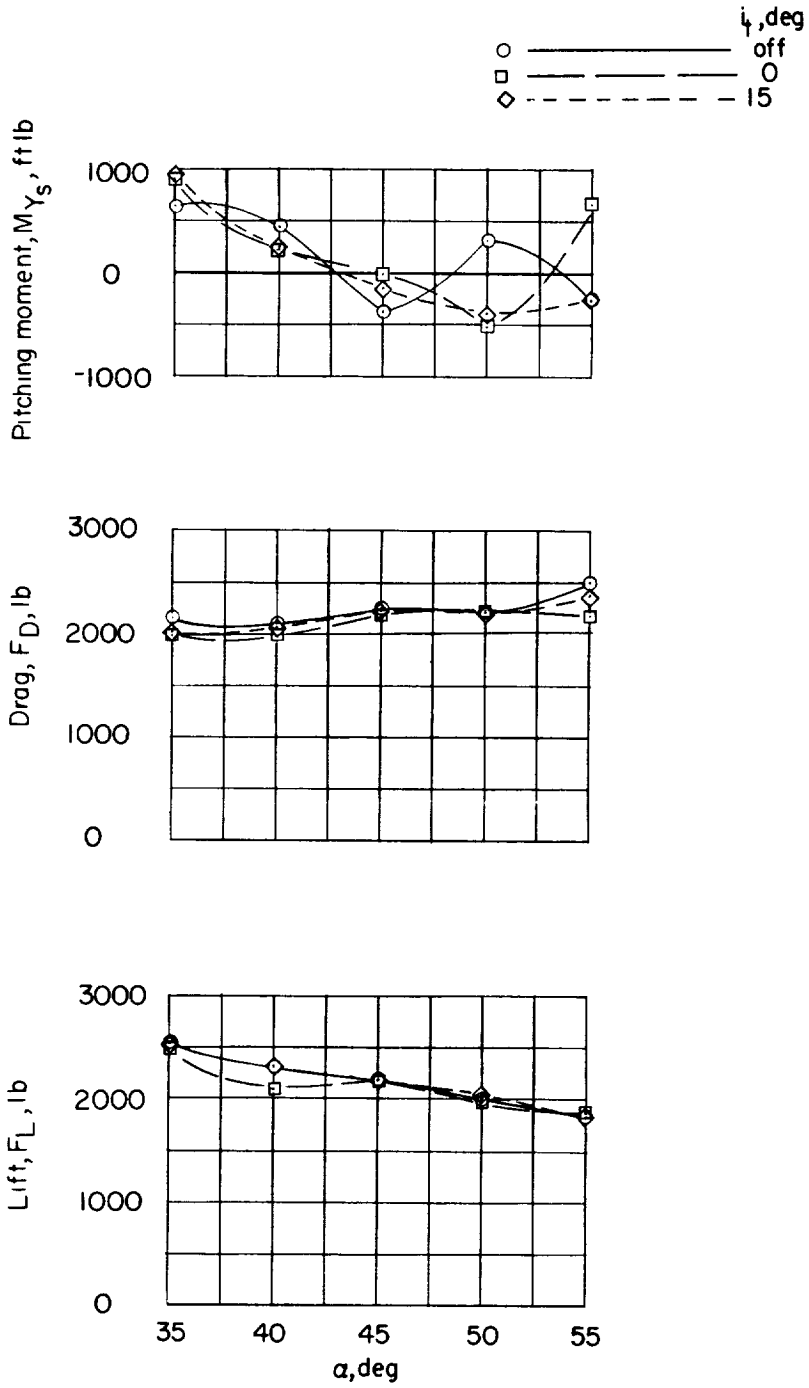

(d) 45° descent at $\alpha = 45°$; V = 31.25 knots.

Figure 9.- Concluded.

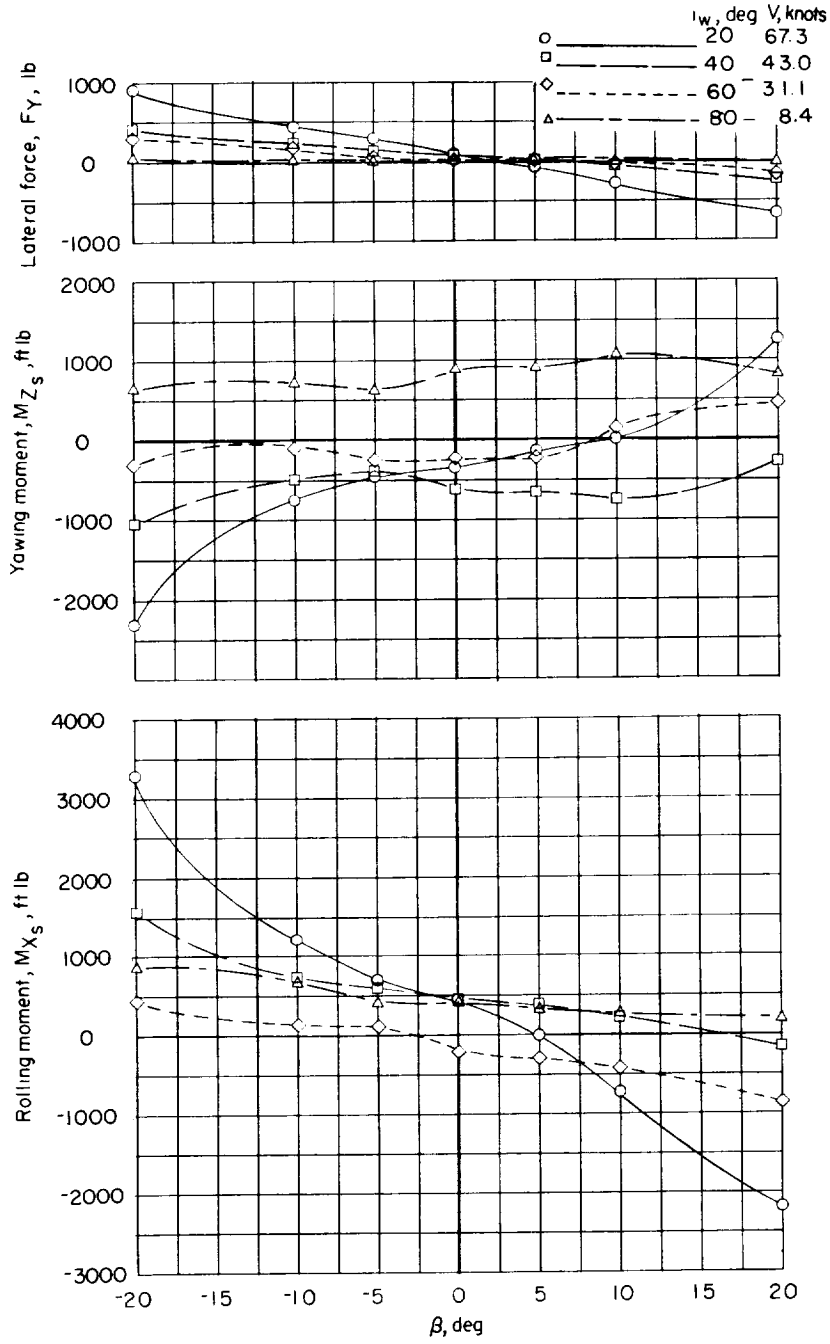

(a) Zero forward acceleration at $\alpha = 0^{\circ}$.

Figure 10.- Lateral stability characteristics in the transition range.

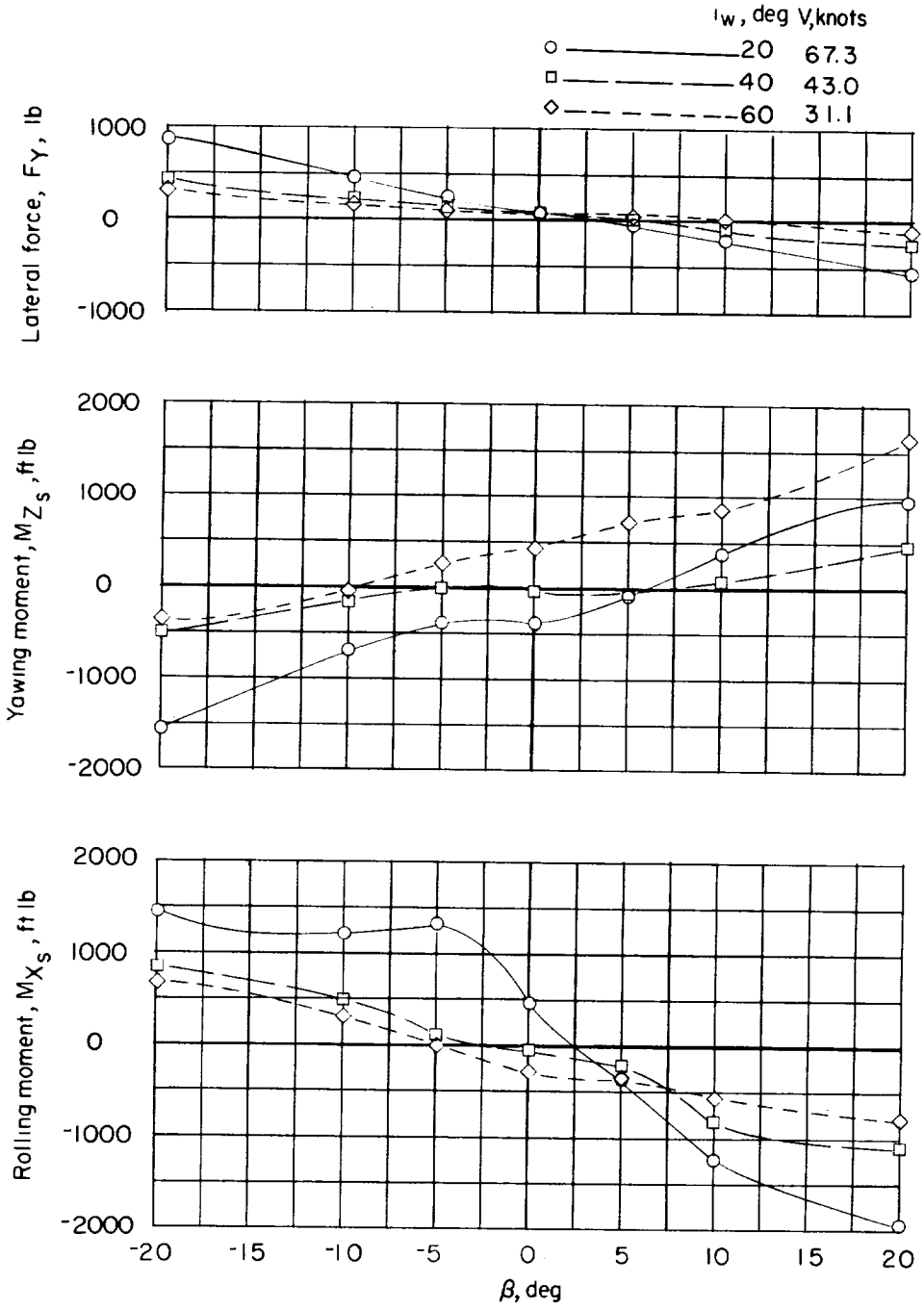

(b) Zero forward acceleration at $\alpha = 10^{\circ}$.

Figure 10.- Continued.

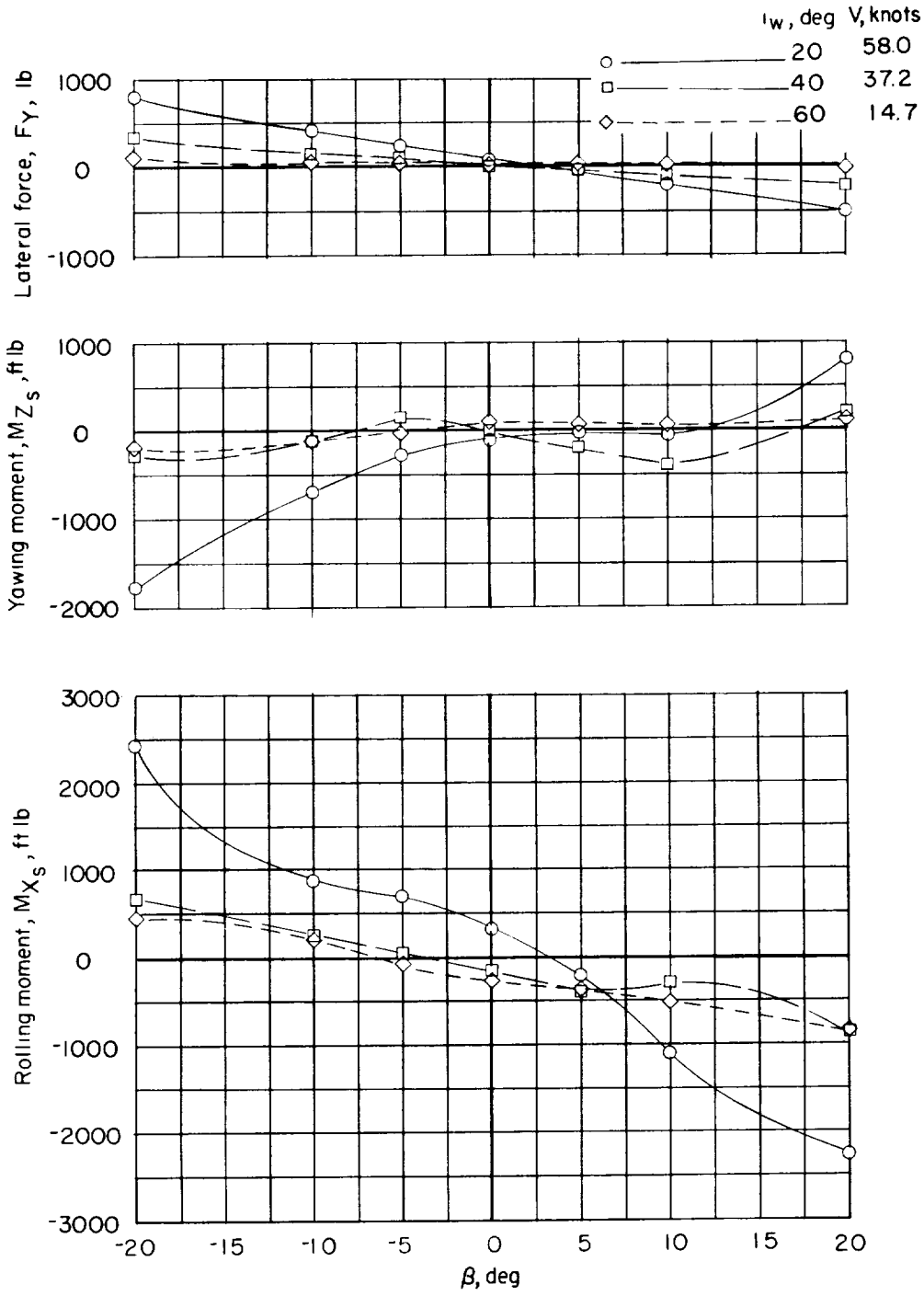

(c) Acceleration of 1/4g at $\alpha = 0^{\circ}$.

Figure 10.- Continued.

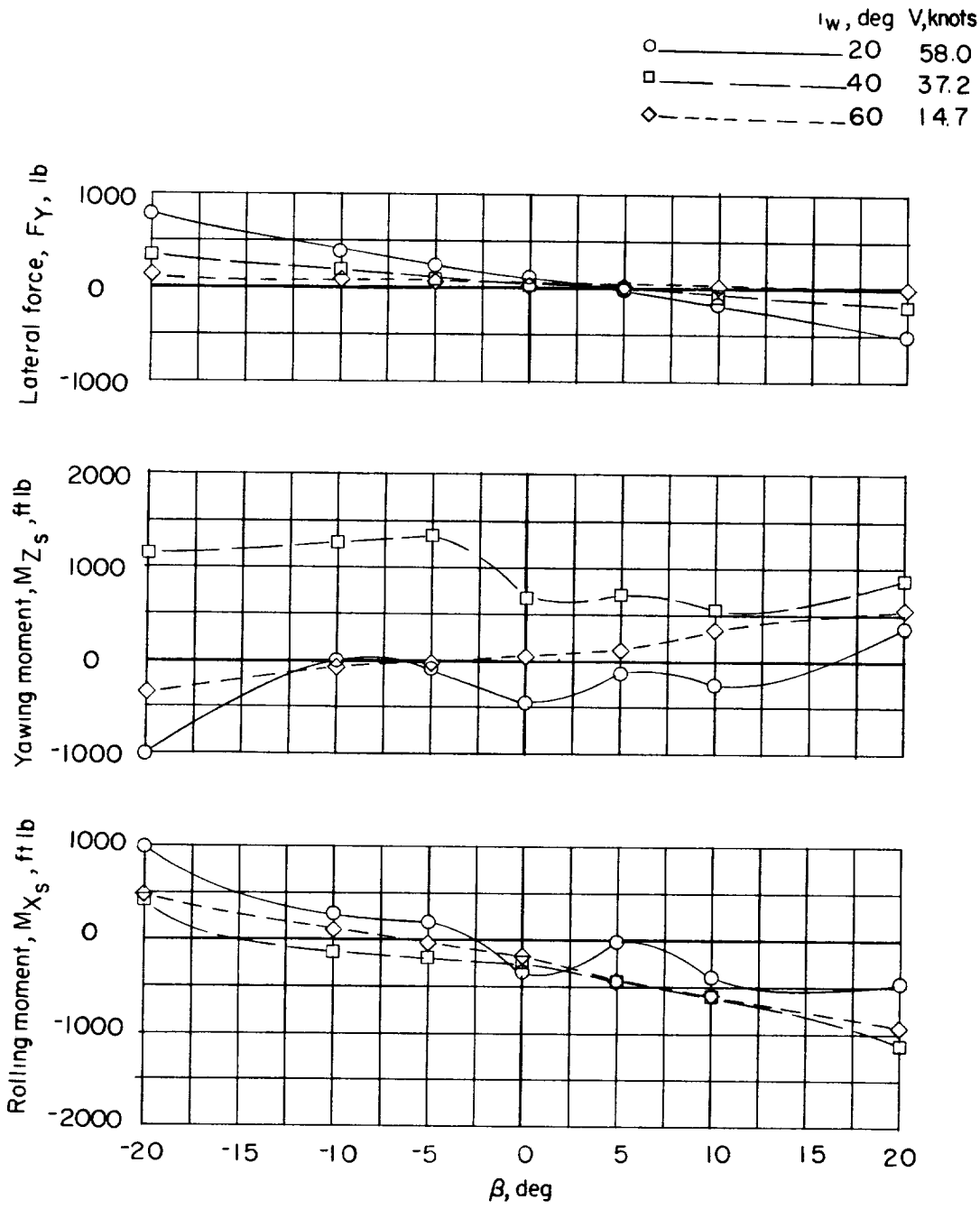

(d) Acceleration of 1/4g at $\alpha = 10^{\circ}$.

Figure 10.- Continued.

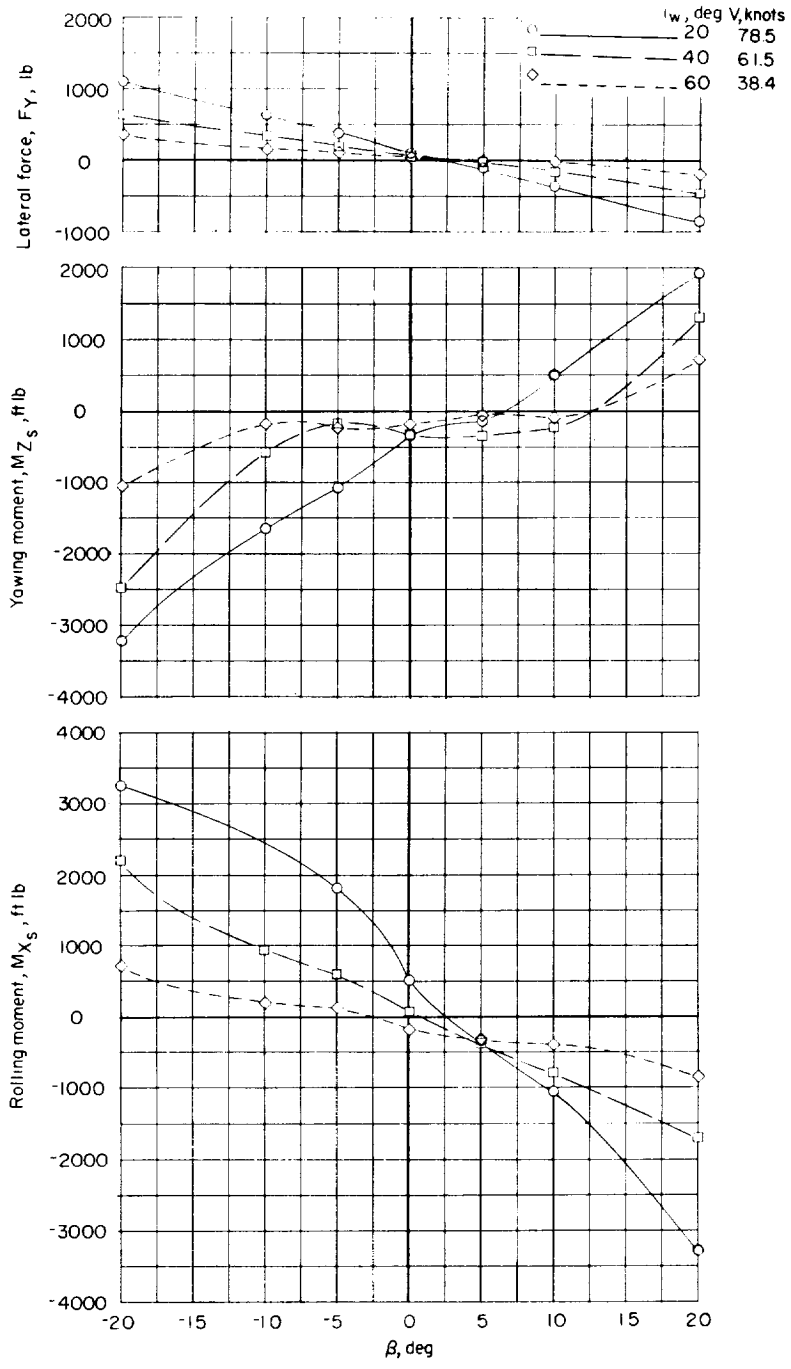

(e) Deceleration of 1/4g at $\alpha = 0^{\circ}$.

Figure 10.- Continued.

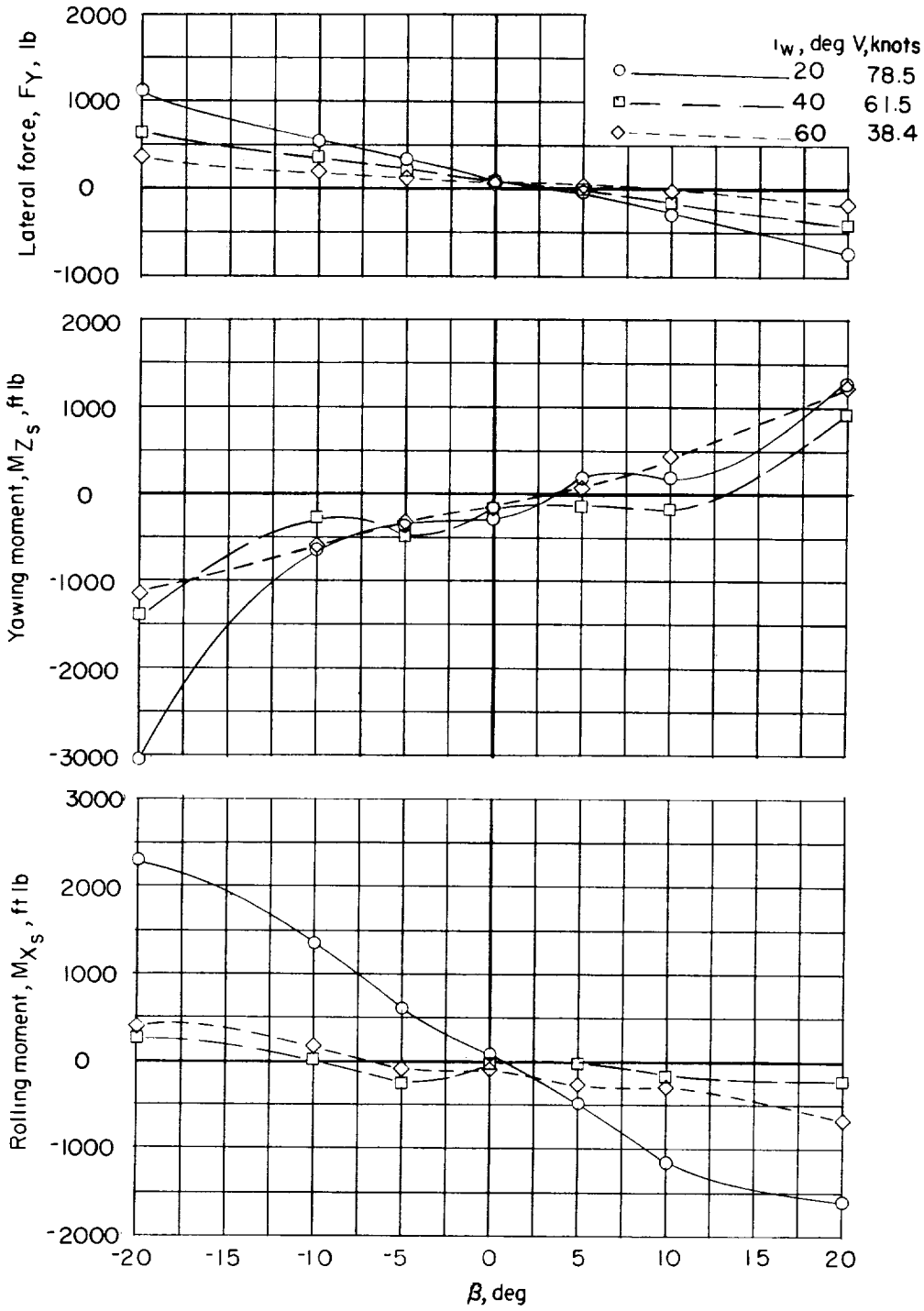

(f) Deceleration of 1/4g at $\alpha = 10^{\circ}$.

Figure 10.- Concluded.

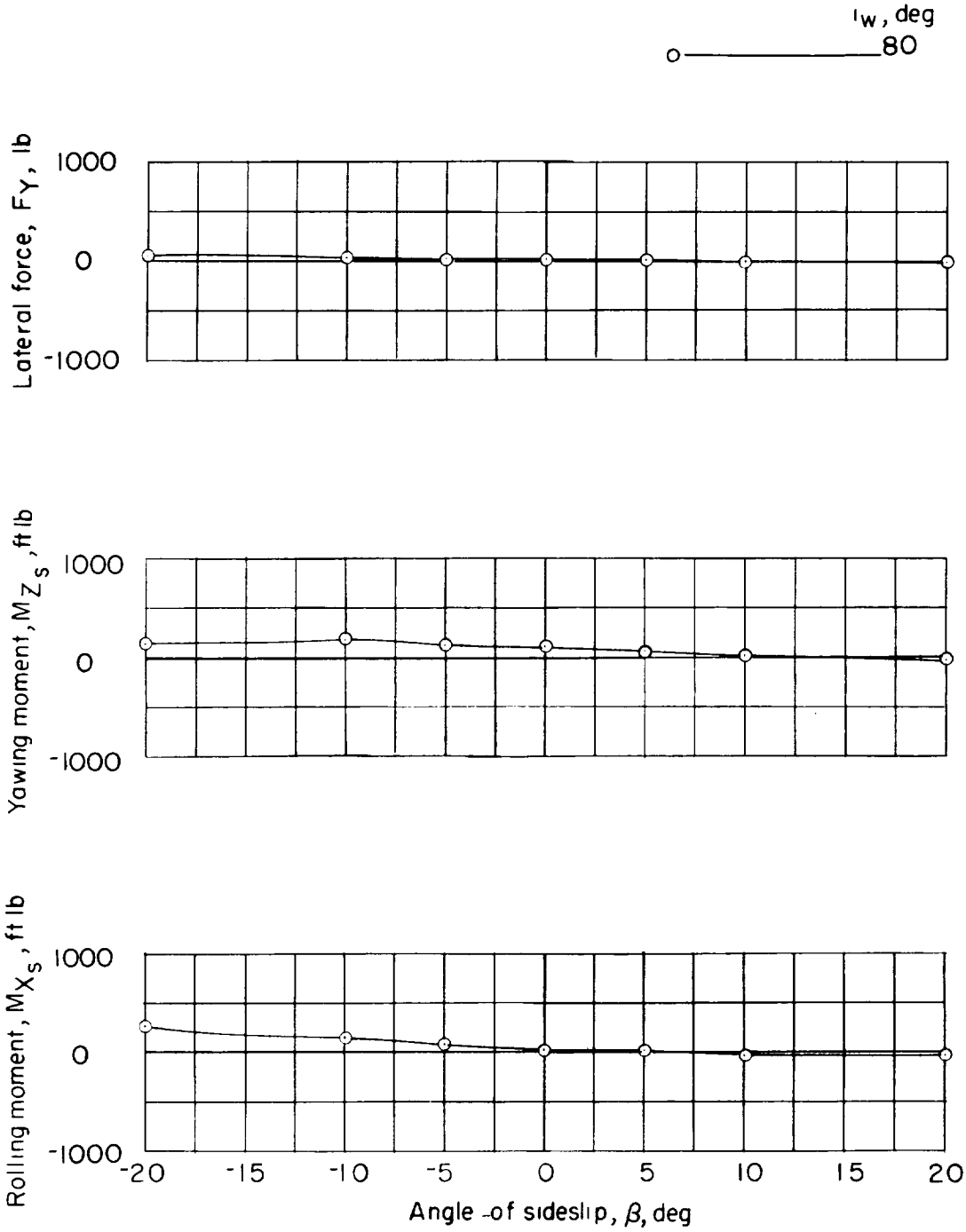

Figure 11.- Lateral stability characteristics in 45° climb. V = 9.27 knots at $i_w = 80°$; $\alpha = -45°$.

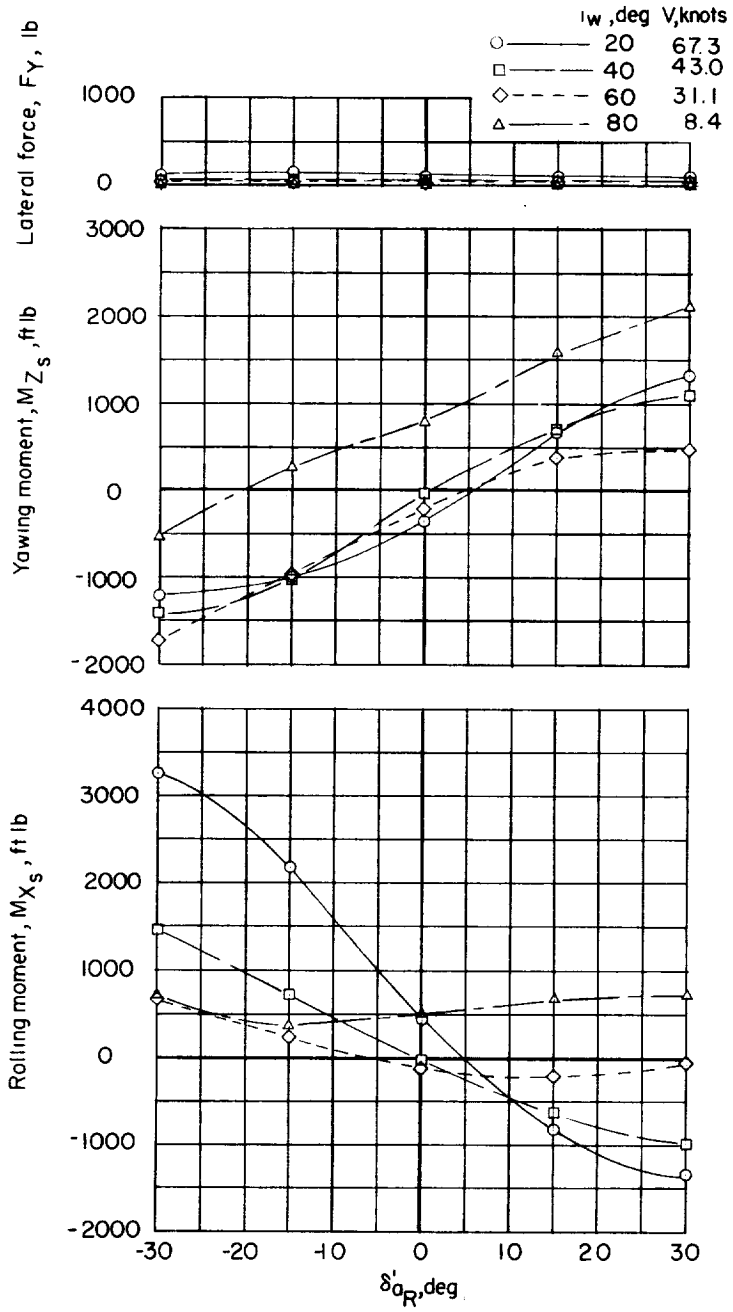

(a) Zero forward acceleration at $\alpha = 0^{\circ}$.

Figure 12.- Aileron effectiveness in the transition range.

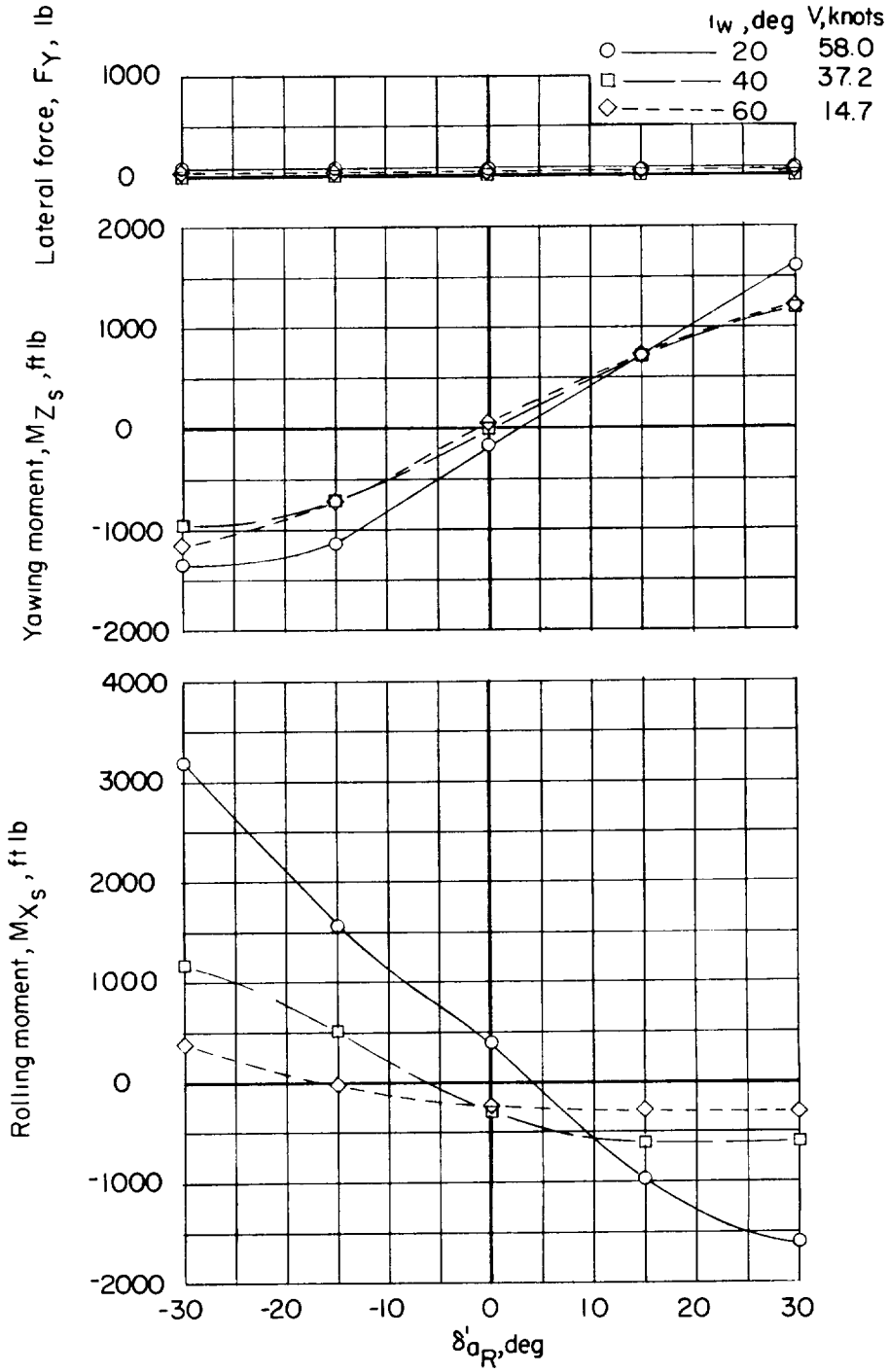

(b) Forward acceleration of 1/4g at $\alpha = 0^\circ$.

Figure 12.- Continued.

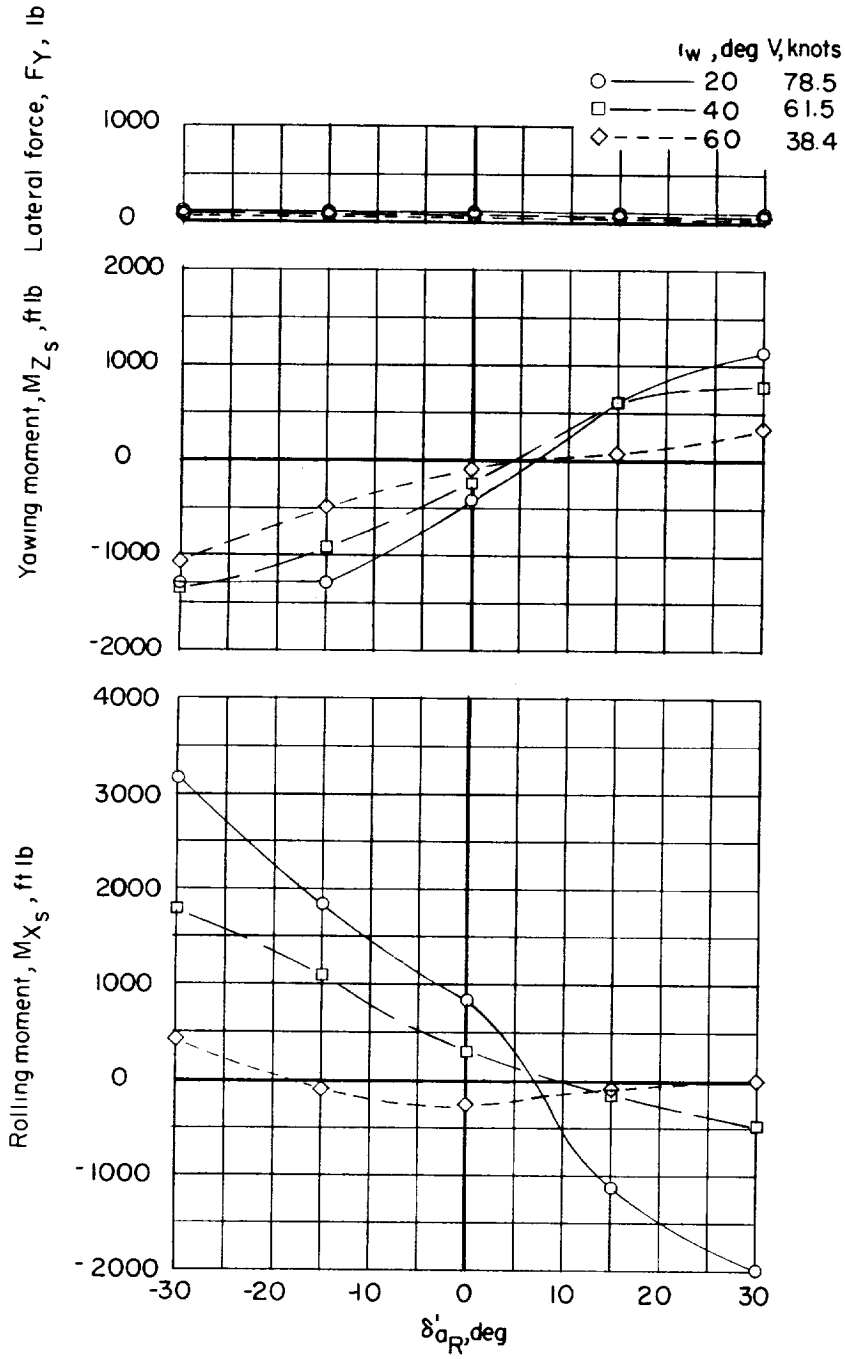

(c) Deceleration of 1/4g at $\alpha = 0^\circ$.

Figure 12.- Concluded.

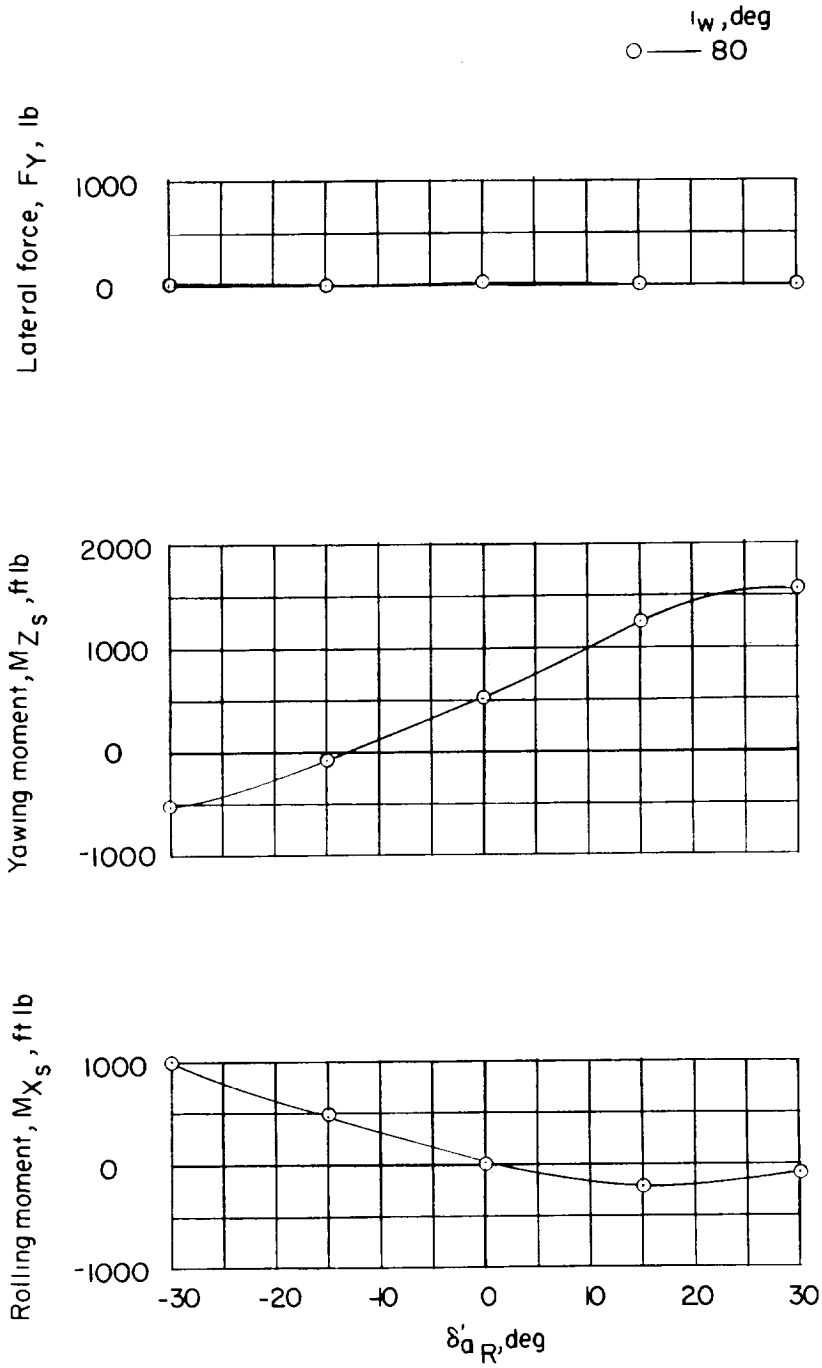

(a) 26.5° climb; α = -26.5°; V = 9.4 knots.

Figure 13.- Aileron effectiveness in 26.5° climb and descent at i_w = 80°.

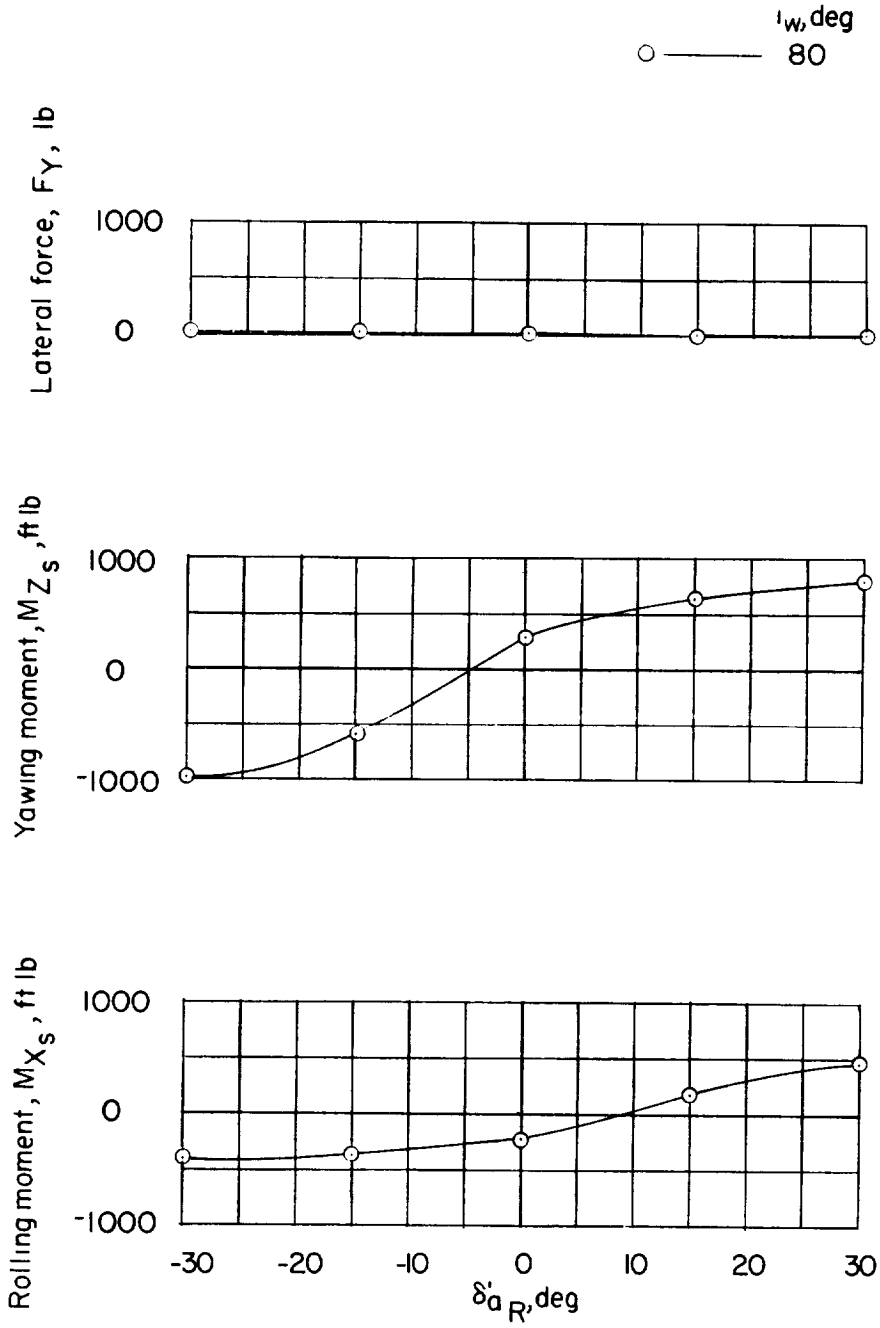

(b) 26.5° descent at α = 26.5°; V = 6.7 knots.

Figure 13.- Concluded.

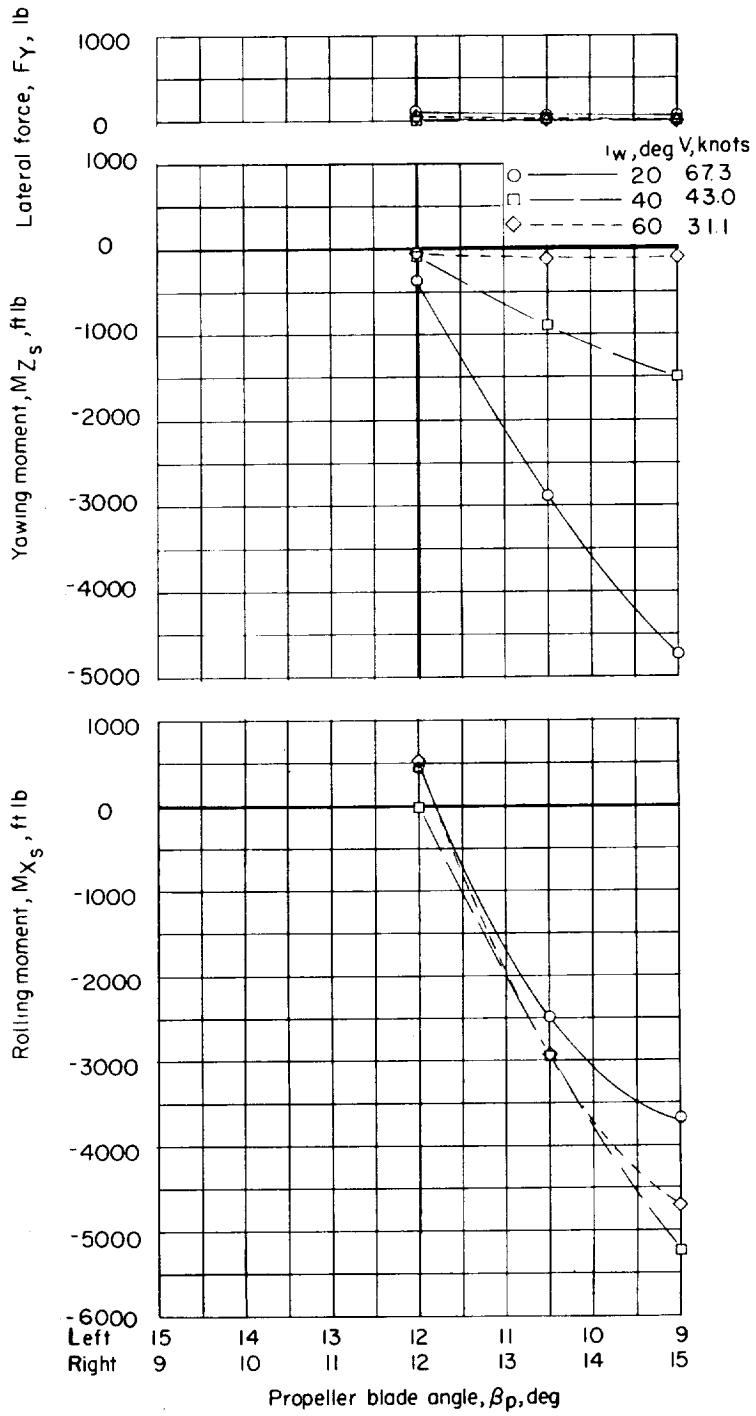

Figure 14.- Effectiveness of differential propeller pitch control with zero forward acceleration at $\alpha = 0^\circ$.

NASA - Langley Field, Va. L-121

NASA MEMO 11-3-58L
National Aeronautics and Space Administration.
FORCE-TEST INVESTIGATION OF THE STABILITY AND CONTROL CHARACTERISTICS OF A 1/4-SCALE MODEL OF A TILT-WING VERTICAL-TAKE-OFF-AND-LANDING AIRCRAFT. William A. Newsom, Jr., and Louis P. Tosti. January 1959. 53p. diagrs., tabs.
(NASA MEMORANDUM 11-3-58L)

The model had two propellers with hinged (flapping) blades mounted on the wing which could be tilted from 4° incidence for forward flight to 86° for hovering flight. The investigation included measurements of both the longitudinal and lateral stability and control characteristics in both the forward flight and transition ranges. Tests in the forward flight condition were made for several values of thrust coefficient and tests in the transition range were made at several values of wing incidence with the power varied to cover a range of flight conditions from

Copies obtainable from NASA, Washington (over)

1. Airplanes - Specific Types (1.7.1.2)
2. Stability, Longitudinal - Static (1.8.1.1.1)
3. Stability, Lateral - Static (1.8.1.1.2)
4. Control, Longitudinal (1.8.2.1)
5. Control, Lateral (1.8.2.2)

I. Newsom, William A., Jr.
II. Tosti, Louis P.
III. NASA MEMO 11-3-58L

NASA

NASA MEMO 11-3-58L
National Aeronautics and Space Administration.
FORCE-TEST INVESTIGATION OF THE STABILITY AND CONTROL CHARACTERISTICS OF A 1/4-SCALE MODEL OF A TILT-WING VERTICAL-TAKE-OFF-AND-LANDING AIRCRAFT. William A. Newsom, Jr., and Louis P. Tosti. January 1959. 53p. diagrs., tabs.
(NASA MEMORANDUM 11-3-58L)

The model had two propellers with hinged (flapping) blades mounted on the wing which could be tilted from 4° incidence for forward flight to 86° for hovering flight. The investigation included measurements of both the longitudinal and lateral stability and control characteristics in both the forward flight and transition ranges. Tests in the forward flight condition were made for several values of thrust coefficient and tests in the transition range were made at several values of wing incidence with the power varied to cover a range of flight conditions from

Copies obtainable from NASA, Washington (over)

1. Airplanes - Specific Types (1.7.1.2)
2. Stability, Longitudinal - Static (1.8.1.1.1)
3. Stability, Lateral - Static (1.8.1.1.2)
4. Control, Longitudinal (1.8.2.1)
5. Control, Lateral (1.8.2.2)

I. Newsom, William A., Jr.
II. Tosti, Louis P.
III. NASA MEMO 11-3-58L

NASA

NASA MEMO 11-3-58L
National Aeronautics and Space Administration.
FORCE-TEST INVESTIGATION OF THE STABILITY AND CONTROL CHARACTERISTICS OF A 1/4-SCALE MODEL OF A TILT-WING VERTICAL-TAKE-OFF-AND-LANDING AIRCRAFT. William A. Newsom, Jr., and Louis P. Tosti. January 1959. 53p. diagrs., tabs.
(NASA MEMORANDUM 11-3-58L)

The model had two propellers with hinged (flapping) blades mounted on the wing which could be tilted from 4° incidence for forward flight to 86° for hovering flight. The investigation included measurements of both the longitudinal and lateral stability and control characteristics in both the forward flight and transition ranges. Tests in the forward flight condition were made for several values of thrust coefficient and tests in the transition range were made at several values of wing incidence with the power varied to cover a range of flight conditions from

Copies obtainable from NASA, Washington (over)

1. Airplanes - Specific Types (1.7.1.2)
2. Stability, Longitudinal - Static (1.8.1.1.1)
3. Stability, Lateral - Static (1.8.1.1.2)
4. Control, Longitudinal (1.8.2.1)
5. Control, Lateral (1.8.2.2)

I. Newsom, William A., Jr.
II. Tosti, Louis P.
III. NASA MEMO 11-3-58L

NASA

NASA MEMO 11-3-58L
National Aeronautics and Space Administration.
FORCE-TEST INVESTIGATION OF THE STABILITY AND CONTROL CHARACTERISTICS OF A 1/4-SCALE MODEL OF A TILT-WING VERTICAL-TAKE-OFF-AND-LANDING AIRCRAFT. William A. Newsom, Jr., and Louis P. Tosti. January 1959. 53p. diagrs., tabs.
(NASA MEMORANDUM 11-3-58L)

The model had two propellers with hinged (flapping) blades mounted on the wing which could be tilted from 4° incidence for forward flight to 86° for hovering flight. The investigation included measurements of both the longitudinal and lateral stability and control characteristics in both the forward flight and transition ranges. Tests in the forward flight condition were made for several values of thrust coefficient and tests in the transition range were made at several values of wing incidence with the power varied to cover a range of flight conditions from

Copies obtainable from NASA, Washington (over)

1. Airplanes - Specific Types (1.7.1.2)
2. Stability, Longitudinal - Static (1.8.1.1.1)
3. Stability, Lateral - Static (1.8.1.1.2)
4. Control, Longitudinal (1.8.2.1)
5. Control, Lateral (1.8.2.2)

I. Newsom, William A., Jr.
II. Tosti, Louis P.
III. NASA MEMO 11-3-58L

NASA

NASA MEMO 11-3-58L

forward acceleration (or climb) conditions to deceleration (or descent) conditions. The data are presented without analysis.

Copies obtainable from NASA, Washington

NASA

NASA MEMO 11-3-58L

forward acceleration (or climb) conditions to deceleration (or descent) conditions. The data are presented without analysis.

Copies obtainable from NASA, Washington

NASA

NASA MEMO 11-3-58L

forward acceleration (or climb) conditions to deceleration (or descent) conditions. The data are presented without analysis.

Copies obtainable from NASA, Washington

NASA

NASA MEMO 11-3-58L

forward acceleration (or climb) conditions to deceleration (or descent) conditions. The data are presented without analysis.

Copies obtainable from NASA, Washington

NASA